UC Davis
UC Davis Previously Published Works

Title
To Break or Not To Break: Sex Chromosome Hemizygosity During Meiosis in Caenorhabditis

Permalink
https://escholarship.org/uc/item/5g68n2r3

Journal
Genetics, 204(3)

ISSN
0016-6731

Authors
Van, Mike V
Larson, Braden J
Engebrecht, JoAnne

Publication Date
2016-11-01

DOI
10.1534/genetics.116.194308

Peer reviewed

eScholarship.org Powered by the California Digital Library
University of California

To Break or Not To Break: Sex Chromosome Hemizygosity During Meiosis in *Caenorhabditis*

Mike V. Van,[1] Braden J. Larson,[2] and JoAnne Engebrecht[3]
Department of Molecular and Cellular Biology, University of California, Davis, California 95616
ORCID ID: 0000-0002-2733-7506 (J.E.)

ABSTRACT Meiotic recombination establishes connections between homologous chromosomes to promote segregation. Hemizygous regions of sex chromosomes have no homologous chromosome to recombine with, yet must be transmitted through meiosis. An extreme case of hemizygosity exists in the genus *Caenorhabditis*, where males have a single X chromosome that completely lacks a homologous partner. To determine whether similar strategies have evolved to accommodate hemizygosity of the X during male meiosis in *Caenorhabditis* with distinct modes of sexual reproduction, we examined induction and processing of meiotic double strand breaks (DSBs) in androdioecious (hermaphrodite/male) *Caenorhabditis elegans* and *C. briggsae*, and gonochoristic (female/male) *C. remanei* and *C. brenneri*. Analysis of the recombinase RAD-51 suggests more meiotic DSBs are induced in gonochoristic *vs.* androdioecious species. However, in late prophase in all species, chromosome pairs are restructured into bivalents around a single axis, suggesting that the holocentric nature of *Caenorhabditis* chromosomes dictates a single crossover per bivalent regardless of the number of DSBs induced. Interestingly, RAD-51 foci were readily observed on the X chromosome of androdioecious male germ cells, while very few were detected in gonochoristic male germ cells. As in *C. elegans*, the X chromosome in *C. briggsae* male germ cells undergoes transient pseudosynapsis and flexibility in DSB repair pathway choice. In contrast, in *C. remanei* and *C. brenneri* male germ cells, the X chromosome does not undergo pseudosynapsis and appears refractory to SPO-11-induced breaks. Together our results suggest that distinct strategies have evolved to accommodate sex chromosome hemizygosity during meiosis in closely related *Caenorhabditis* species.

KEYWORDS double strand breaks (DSBs); meiosis; RAD-51; sex chromosomes; synapsis; Genetics of Sex

MEIOSIS is essential for sexual reproduction and involves the precise halving of the genome for packaging into gametes. Meiosis relies on homology between maternal and paternal chromosomes to form physical connections for accurate chromosome segregation (reviewed in Zickler and Kleckner 2015). While the overall meiotic program is similar between the sexes, meiosis is sexually dimorphic with respect to timing, the recombination landscape, and mechanisms of meiotic chromosome segregation (reviewed in Morelli and Cohen 2005). Additionally, the presence of differentiated sex chromosomes in the heterogametic sex contributes to differences in female and male meiosis. Heterogametic sex chromosomes have limited or no homology, but as with the autosomes must be accurately transmitted to the next generation.

In meiotic cells, both autosomes and sex chromosomes exists in an environment where recombination is actively engaged to ensure the formation of crossovers. Meiotic recombination is initiated by DNA double strand breaks (DSBs) mediated by the conserved topoisomerase Spo11 and associated proteins (Keeney *et al.* 1997; Dernburg *et al.* 1998; Cole *et al.* 2010; Rosu *et al.* 2013; Stamper *et al.* 2013). Meiotic DSBs are processed to promote homologous recombination (HR). Central to HR, is break resection (Penkner *et al.* 2007; Garcia *et al.* 2011; Lemmens *et al.* 2013; Yin and Smolikove 2013) and loading of recA recombinases RAD51/DMC1, which mediate strand invasion (Bishop *et al.* 1992; Alpi *et al.* 2003; Brown and Bishop 2015). A subset of processed breaks is converted into crossovers, which require unique molecular machinery and provide the physical connection between homologs. Recent work has established that crossover formation is exquisitely controlled and involves both

Copyright © 2016 by the Genetics Society of America
doi: 10.1534/genetics.116.194308
Manuscript received July 30, 2016; accepted for publication September 6, 2016; published Early Online September 7, 2016.
Supplemental material is available online at www.genetics.org/lookup/suppl/doi:10.1534/genetics.116.194308/-/DC1.
[1]Present address: Stanford University, Stanford, CA.
[2]Present address: University of California, Santa Cruz, CA.
[3]Corresponding author: Department of Molecular and Cellular Biology, University of California, One Shields Ave., Davis, CA 95616. E-mail: jengebrecht@ucdavis.edu

repair in the context of the specialized meiotic chromosome structure and regulatory mechanisms to monitor DSB formation, processing, and ultimately, crossover formation (Shinohara *et al.* 2008; Rosu *et al.* 2011, 2013; Stamper *et al.* 2013; Yu *et al.* 2016).

Our understanding of how meiosis in general, and sex chromosomes specifically, is differentially regulated in the sexes is limited to the small number of model organisms where it has been examined mechanistically, most notably in *Mus musculus*, *Drosophila melanogaster*, and *C. elegans*. Each of these organisms uses a different strategy for accommodating sex chromosomes during meiosis, suggesting that these strategies arose independently in concert with the emergence of sex chromosomes in the different lineages. For example, in mice the obligate crossover at the homologous pseudoautosomal region (PAR) between the X and the Y requires a specific isoform of Spo11 and specialized chromosome structure (Kauppi *et al.* 2011). On the other hand, in *Drosophila* males, meiosis is achiasmatic and thus does not rely on meiotic recombination at all; however, pairing and segregation of the X–Y sex chromosomes is dependent on ribosomal DNA homology between the chromosomes (McKee 1996).

The nematode, *C. elegans*, represents an extreme example of hemizygosity as the X chromosome of males completely lacks a pairing partner. Further, as in mammals, the X chromosome is transcriptionally silenced by meiotic sex chromosome inactivation (Kelly *et al.* 2002; Reuben and Lin 2002; Bean *et al.* 2004; Checchi and Engebrecht 2011). We previously reported that the X chromosome of *C. elegans* males undergoes a brief period of pseudosynapsis, [*i.e.*, apparent synapsis that does not necessarily constitute full alignment or contain all components of the synaptonemal complex (SC)] concurrent with the formation of SPO-11-dependent DSBs (Checchi *et al.* 2014). However, the X chromosome is refractory to DSB feedback mechanisms, which control and regulate recombination on the autosomes. Further, unlike autosomes, X-specific breaks can be repaired in the absence of HR (Checchi *et al.* 2014), suggesting alternative DSB repair pathways can be engaged. *C. elegans* is one member of a large and diverse family of nematodes, with distinct modes of sexual reproduction and occupying wide ecological niches (Kiontke and Fitch 2005; Kiontke *et al.* 2011). Whether the same strategies are used in other *Caenorhabditis* species is not known. Here we compare meiotic DSB patterns genome-wide and on the X chromosome in *Caenorhabditis* species that are hermaphroditic/male or obligate female/male. We find strikingly different strategies for sex chromosome transmission among these closely related *Caenorhabditis* species, suggesting a remarkable degree of divergence in the behavior of hemizygous sex chromosomes during meiosis even within the same lineage.

Materials and Methods

Genetics

Strains were maintained at 20° unless otherwise noted. *C. elegans* var. Bristol (N2), *C. briggsae* (AF16), *C. remanei* (SB146), *C. brenneri* (CB5161), *C. nigoni* (JU1325), and *C. tropicalis* (JU1373) were used as the wild-type strain for each respective species. *C. briggsae* and *C. remanei* RNA interference (RNAi) sensitive by feeding strains JU1018:*mfIs42*[*Cel-sid-2* + *Cel-myo-2*::DsRed] and JU1184:*mfEx34*[*Cel-sid-2* + *Cel-myo-2*::DsRed] were generated by Nuez and Felix (2012). All experiments were performed on animals maintained at a ratio of one female/hermaphrodite to three males. Some nematode strains used in this work were provided by the *Caenorhabditis* Genetics Center, which is funded by the National Institutes of Health (NIH) National Center for Research Resources.

Embryonic lethality was determined by counting eggs and hatched larvae 24 hr after removing adult and calculating percentage as eggs/eggs + larvae.

Cytological analysis

Immunostaining of germ lines was performed as described (Jaramillo-Lambert *et al.* 2007). The following primary antibodies were purchased and used at the indicated dilutions: mouse anti-histone H3K4me2 (1:500; catalog no. 05-1338) and rabbit anti-pH 3S10 (1:500; catalog no. 06-570) (Millipore, Temecula, CA); rabbit anti-RAD-51 (1:10,000; catalog no. 29480002) (Novus Biologicals, Littleton, CO); and mouse anti-nuclear pore complex proteins (Mab414) (1:250; catalog no. ab24609) (Abcam, Cambridge, MA). Rabbit anti-AIR-2 (1:500) was generously provided by Jill Schumacher (University of Texas) and rat anti-RAD-51 (1:100) was generously provided by Anne Villeneuve (Stanford University). Goat anti-SYP-1 (1:250) and rabbit anti-SYP-2 (1:250) were generous gifts from Sarit Smolikove (University of Iowa). The following secondary antibodies from Life Technologies were all used at 1:500 dilutions: Alexa Fluor 594 donkey anti-mouse IgG, Alexa Fluor 488 goat anti-mouse IgG, Alexa Fluor 596 donkey anti-rabbit IgG, Alexa Fluor 488 donkey anti-rabbit IgG, Alexa Fluor 488 donkey anti-goat IgG, and Alexa Fluor 555 goat anti-rat IgG. Alexa Fluor 647 goat anti-rabbit was used at 1:250 dilution. DAPI (2 μg/ml; Sigma, St. Louis, MO) was used to counterstain DNA.

Collection of images was performed using an API Delta Vision deconvolution microscope or Nikon Instruments Eclipse Ti-E microscope. A minimum of three germ lines was examined for each condition and experiments were repeated a minimum of three times. Images were deconvolved using Applied Precision SoftWoRx or Huygens imaging analysis software and subsequently processed and analyzed using Fiji (ImageJ) (Wayne Rasband, NIH).

RAD-51 foci were quantified in three germ lines of age-matched hermaphrodites/females or males (24 hr post-L4). A single gonadal arm was scored in hermaphrodites/females. Germ lines were divided by meiotic prophase substage based on morphology and position; transition zone was counted from the first row with three or more crescent-shaped nuclei until the last row with three or more crescent-shaped nuclei, and pachytene was divided into three equal sections for early (EP), mid (MP), and late pachytene (LP). The number of foci per nucleus was scored for each stage. Quantification of RAD-51 foci specific

to the X chromosome(s) was scored as foci that localized to the chromosome that lacked the activating mark H3K4me2.

RNAi analysis

RNAi experiments were performed at 20°, using the feeding method (Timmons *et al.* 2001). *C. briggsae* or *C. remanei* L4 hermaphrodites/females were mated with mix-staged males. After 24 hr, hermaphrodites/females with mating plugs were transferred onto RNAi plates. The hermaphrodite/female and male progeny that grew up on the RNAi plates were transferred to a second RNAi plate and the resultant progeny were analyzed for progeny viability as well as by antibody staining of dissected germ lines. *Cbr-rad-51*, *Cbr-rad-54*, and *Cbr-spo-11* sequences were isolated from AF16 genomic DNA and *Cre-rad-51.2* and *Cre-spo-11* were isolated from SB146 genomic DNA. The resulting PCR fragments were inserted into the L4440 vector by Gibson assembly. Primers used for cloning are listed in Supplemental Material, Table S1. Cultures were plated onto NGM plates containing 25 μg/ml carbenicillin and 1 mM IPTG and were used within 2 weeks.

Irradiation treatment

For experiments assessing formation of RAD-51 foci following irradiation (IR) treatment, 24 hr post-L4 worms were exposed to 10–30 Gy of γ-irradiation from a ^{137}Cs source; gonads were dissected and fixed for immunofluorescence as above, at 30 min to 8 hr post-IR.

Data and regeant availability

Plasmids generated and complete imaging data sets are available upon request.

Results

Patterns of genomewide RAD-51 are similar in closely related Caenorhabditis species

The spatiotemporal organization of the *C. elegans* germ line has facilitated cytological analyses of recombination as all stages of meiotic prophase are present and readily visualized within a single animal (Shakes *et al.* 2009; Lui and Colaiácovo 2013) (Figure 1, A and D). Specifically, the loading and disassembly of the recombinase RAD-51 by immunostaining has served as a proxy for ongoing meiotic DSB repair. SPO-11-dependent RAD-51 foci are first detected in early prophase (transition zone, TZ), peak in EP to MP, and are largely disassembled by LP (Colaiácovo *et al.* 2003). While the overall pattern of RAD-51 foci is similar in hermaphrodite and male germ lines, RAD-51 foci peak earlier in male germ cells (Jaramillo-Lambert and Engebrecht 2010; Checchi *et al.* 2014) (Figure 1).

To monitor meiotic DSB repair in *Caenorhabditis* species, we examined the localization of RAD-51 by immunostaining in germ lines of *C. elegans* and *C. briggsae*, two lineages that independently evolved hermaphrodism, and the obligate female/male species, *C. remanei* and *C. brenneri*. The organization of the germ line is conserved in these species, allowing for comparison of RAD-51 assembly and disassembly (Figure 1A and Figure S2), although there are differences in numbers of nuclei at the different meiotic prophase substages (Larson *et al.* 2016). Consequently, we scored the number of RAD-51 foci/nucleus in each zone and compared this number between the species (Figure 1 and Figure S3). We found the overall pattern of RAD-51 loading and removal to be similar between all of the species; very low numbers of RAD-51 foci were observed in the proliferative zone (PZ) and entry into meiosis (TZ) marked an increase in RAD-51 foci, which peaked at EP during oogenesis and at TZ to EP during spermatogenesis (Figure 1, B, C, E, and F and Figure S3, A and B). Further, RAD-51 declined to very low levels by LP in all species, except in *C. remanei* females, where substantial numbers of RAD-51 were still observed in LP but were reduced by diplotene (Figure 1, B, C, E, and F and Figure S3).

The pattern of RAD-51 appearance and disappearance is consistent with the hypothesis that we are monitoring meiotic DSBs in these other species as has been demonstrated in *C. elegans* hermaphrodites (Colaiácovo *et al.* 2003) and males (Jaramillo-Lambert and Engebrecht 2010). To confirm this, we used *C. briggsae* and *C. remanei* strains expressing *C. elegans* SID-2 from an integrated chromosomal array, which makes them susceptible to RNAi by feeding (Nuez and Felix 2012), and grew the corresponding worms in the presence of *Cbr-spo-11*, *Cre-spo-11*, *Cbr-rad-51*, or *Cre-rad-51.2* double stranded RNA (dsRNA). *Cbr-spo-11*(RNAi) and *Cbr-rad-51*-(RNAi) worms grown for two generations in the presence of dsRNA had elevated levels of embryonic lethality (embryonic lethality: *Cbr*-WT (L4440 control) = 2.7 ± 0.8%; *Cbr-spo-11*(RNAi) = 39.3 ± 5.8%, $P < 0.01$; *Cbr-rad-51*(RNAi) = 99 ± 1.5%, $P < 0.0001$) and greatly reduced levels of RAD-51 foci within both the *C. briggsae* hermaphrodite (data not shown) and male germ lines (Figure 1G), indicating that we are specifically monitoring SPO-11-induced meiotic DSBs loaded with RAD-51. For *C. remanei*, *spo-11*(RNAi) did not result in a reduction in either progeny viability or RAD-51 foci (data not shown), suggesting that the RNAi was not efficient. On the other hand, *Cre-rad-51.2*(RNAi) worms had elevated levels of embryonic lethality (embryonic lethality: *Cre*-WT (L4440 control) = 14.4 ± 5.6% *vs.* *Cre-rad-51.2*(RNAi) = 61.8 ± 8.3%, $P = 0.0007$) and female germ lines had reduced levels of RAD-51 foci (Figure 1H). Together, the observed pattern of RAD-51 foci in the germ line in all of the species along with the demonstrated specificity of the RAD-51 antibody in *C. briggsae* and *C. remanei*, suggest that RAD-51 immunostaining can be used as a readout of meiotic DSB repair in *Caenorhabditis*.

While the overall patterns are similar, the female/male species had significantly more RAD-51 foci throughout meiotic prophase during both oogenesis and spermatogenesis than the hermaphrodite/male species (Figure 1, C and F, compare red and blue lines, and Figure S3 and Figure S4). Consistent with elevated RAD-51 levels being correlated with gonochorism, *C. nigoni*, a sister species of *C. briggsae* (Woodruff *et al.* 2010; Kiontke *et al.* 2011), also had high

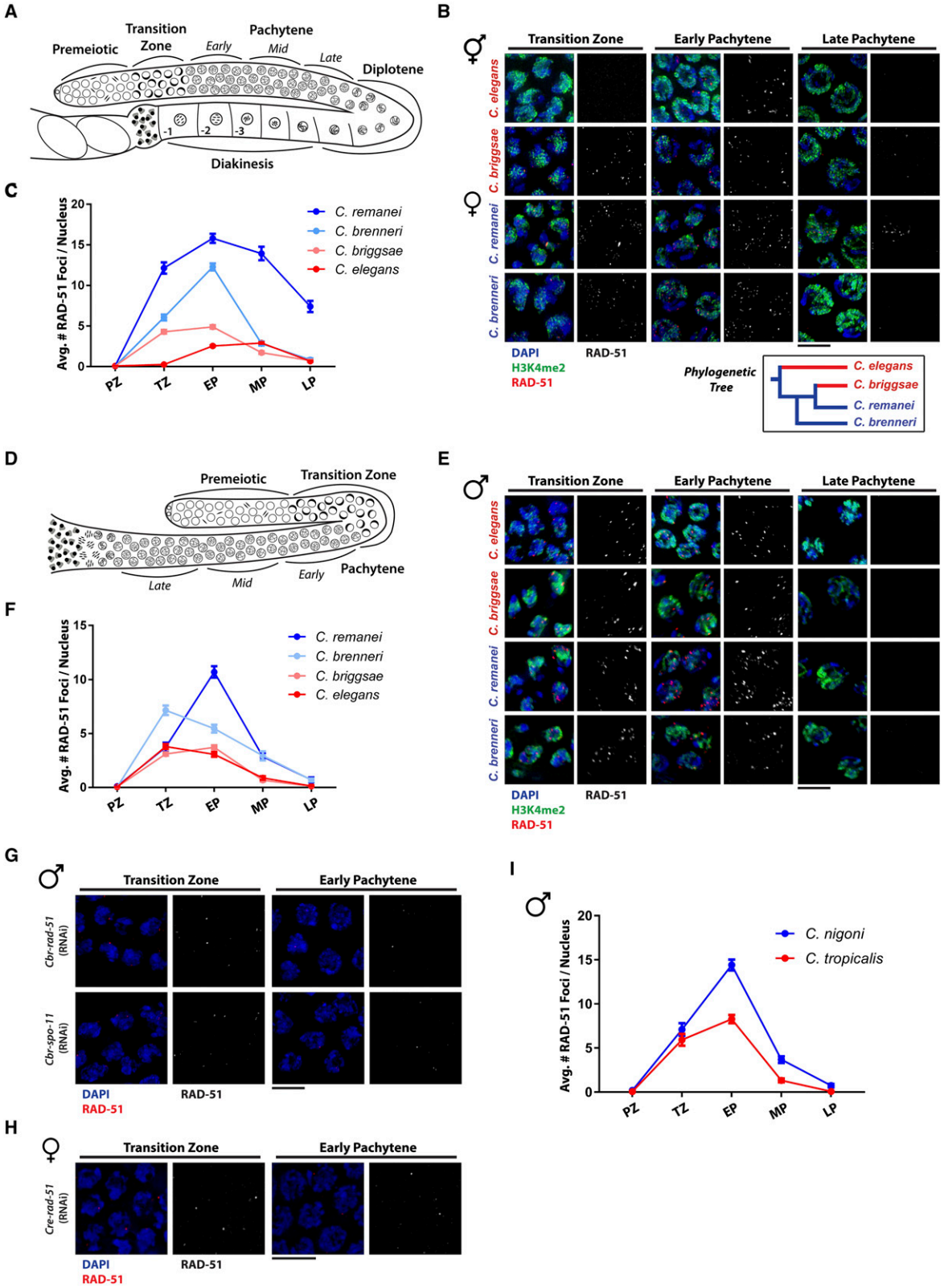

Figure 1 RAD-51 as a readout for DNA break repair in *Caenorhabditis* species. (A and D) Diagrams of the spatiotemporal organization of the hermaphrodite (A) and male (D) *Caenorhabditis* germ lines. Female *Caenorhabditis* germ lines look the same except that they do not make sperm. (B and E) *C. elegans*, *C. briggsae*, *C. remanei*, and *C. brenneri* female/hermaphrodite and male pachytene nuclei stained with DAPI (blue), anti-H3K4me2 (green), and RAD-51 (red). (B) Below is the phylogenetic relationship between the species (redrawn from Kiontke *et al.* 2011). (C and F) Comparison of average number of RAD-51 foci/nucleus at the premeiotic; proliferative zone (PZ), transition zone (TZ), early pachytene (EP), mid pachytene (MP), and

numbers of RAD-51 foci, while the other hermaphrodite/male species in the *elegans* group, *C. tropicalis*, had low levels of RAD-51 foci (Figure 1I). Thus, female/male species appear to have overall higher numbers of DSBs as monitored by RAD-51.

Conservation of bivalent restructuring suggests a single crossover is formed per chromosome pair in Caenorhabditis

In all organisms where they have been examined, many more meiotic DSBs are induced than will be processed into crossovers (reviewed in Lake and Hawley 2016). In *C. elegans*, a single, off-centered crossover is formed on most chromosome pairs, presumably due to the holocentric nature of the chromosomes (Albertson *et al.* 1997; Hillers and Villeneuve 2003; Hammarlund *et al.* 2005). The position of the crossover dictates the restructuring of the bivalent into a long and short arm for regulated cohesion release and accurate chromosome segregation (Nabeshima *et al.* 2005; de Carvalho *et al.* 2008). As the *Caenorhabditis* genus is holocentric (Coghlan 2005; Zedek and Bures 2012), it is likely that a single crossover is formed even in the female/male species where we observed significantly more RAD-51 foci. Consistent with this, two-lobed bivalents at diakinesis resembled those in *C. elegans* (Figure 2). To probe the organization of the bivalent, we stained oogenic germ lines from all four species with antibodies directed against *Cel*-AIR-2 (Aurora B kinase ortholog) (Figure S1B) and examined diakinesis oocytes (−3, −2, −1 position from the spermatheca; Figure 1A). Aurora B is important for regulated cohesin release and specifically marks the short arm of the bivalent (Kaitna *et al.* 2002; Rogers *et al.* 2002; de Carvalho *et al.* 2008). We observed discrete AIR-2 staining at the interface between the bivalent lobes in *C. elegans*, *C. briggsae*, and *C. remanei*, which presumably represent the short arm (Figure 2, A and B). However, the timing of AIR-2 localization at the midbivalent was distinct: in *C. elegans*, AIR-2 was observed on the short arms beginning in the −2 oocyte, in *C. briggsae* it was only apparent in the −1 oocyte, and in *C. remanei*, AIR-2 was evident at the midbivalent region in −3 to −1 oocytes (Figure 2A). *C. brenneri* AIR-2 is 69% identical to *Cel*-AIR-2 (*vs. C. briggsae* 82% and *C. remanei* 80%) and displays no identity with the region used for antibody production (Figure S1B); consequently, no specific staining was observed with the *Cel*-AIR-2 antibodies. To probe the bivalent structure of *C. brenneri* oocytes, we stained oogenic germ lines with antibodies that recognize the phosphorylated form of histone 3 serine 10 (pH3S10), which is phosphorylated by AIR-2 (Hsu *et al.* 2000). Histones are highly conserved and pH3S10 has previously been shown to also be concentrated on the short arm of the bivalent in *C. elegans* oocytes (Collette *et al.* 2011). pH3S10 was exclusively on the short arm of bivalents in *C. elegans*, concentrated on the bivalent short arms in *C. remanei* and *C. brenneri* oocytes and detectable on the short arm of bivalents in *C. briggsae* oocytes. Additionally, and in contrast to *C. elegans*, different extents of pH3S10 were detected around the entire bivalent in these other species (Figure 2C), suggesting additional kinases may be phosphorylating H3S10 and/or that AIR-2 is present around the bivalent below detectable levels. LAB-1, a marker for the long arm (de Carvalho *et al.* 2008), is poorly conserved among the species (40–48% identity with *Cel*-LAB-1) precluding analysis. Nonetheless, these results suggest that chromosomes are restructured into a short and long arm consistent with formation of a single crossover on each chromosome pair in all species.

In *C. elegans*, central components of the SC are asymmetrically disassembled during late prophase and retained on the short arm of bivalents in the −3 oocyte (de Carvalho *et al.* 2008). To further examine restructuring of the bivalent, we monitored the disassembly of SC central components in all four species at LP using anti-peptide antibodies generated against *C. elegans* SYP-1, which also recognizes *C. remanei* and *C. brenneri* SYP-1 and *C. elegans* SYP-2, which also recognizes *C. briggsae* SYP-2 (Figure S1, C and D) (Larson *et al.* 2016). As all SYPs are interdependent for SC assembly (Colaiácovo *et al.* 2003; Smolikov *et al.* 2007b, 2009), we hypothesized that all would behave the same, even though we were limited to examining a single SYP in each species due to the extent of SYP identity between the species. In *C. briggsae*, SYP-2 was partially disassembled in diplotene and appeared to be retained at the intersection between some of the homologous chromosome pairs in −3 oocytes (Figure 2, D and E). Note that the chromosome pairs appear very extended at this stage in *C. briggsae*. In both *C. elegans* and *C. briggsae*, no SYP-2 was detected on −2 oocyte chromosomes. In contrast to *C. elegans* and *C. briggsae*, we did not observe asymmetric removal of SYP-1 in *C. remanei* or *C. brenneri* at the corresponding stages of meiotic prophase. In *C. remanei*, SYP-1 was largely removed from chromosomes in diplotene and formed a SYP-1 aggregate/polycomplex not associated with chromatin in −3 oocytes (Figure 2D, yellow arrows). In *C. brenneri*, SYP-1 was partially removed by diplotene and no SYP-1 was observed in the −3 oocyte. These results suggest that while bivalents are restructured, there are differences in SC disassembly among these *Caenorhabditis* species.

Levels of X-specific RAD-51 foci are strikingly different in C. elegans and C. briggsae vs. C. remanei and C. brenneri male germ cells

During *C. elegans* meiosis, X chromosomes have several unique properties, including accumulation of repressive chromatin marks, transcriptional silencing, and alteration of the

late pachytene (LP) for each *Caenorhabditis* species. A minimum of three germ lines were examined for each species. Error bars = SEM. (G) TZ and EP nuclei stained with DAPI (blue) and anti-RAD-51 (red) from *C. briggsae* males treated with indicated RNAi. (H) TZ and EP nuclei stained with DAPI (blue) and anti-RAD-51 (red) isolated from *C. remanei* females treated with *Cre-rad-51* dsRNA. (I) Comparison of average number of RAD-51 foci/nucleus during PZ, TZ, EP, MP, and LP for *C. nigoni* and *C. tropicalis* males. All bars, 5 μM.

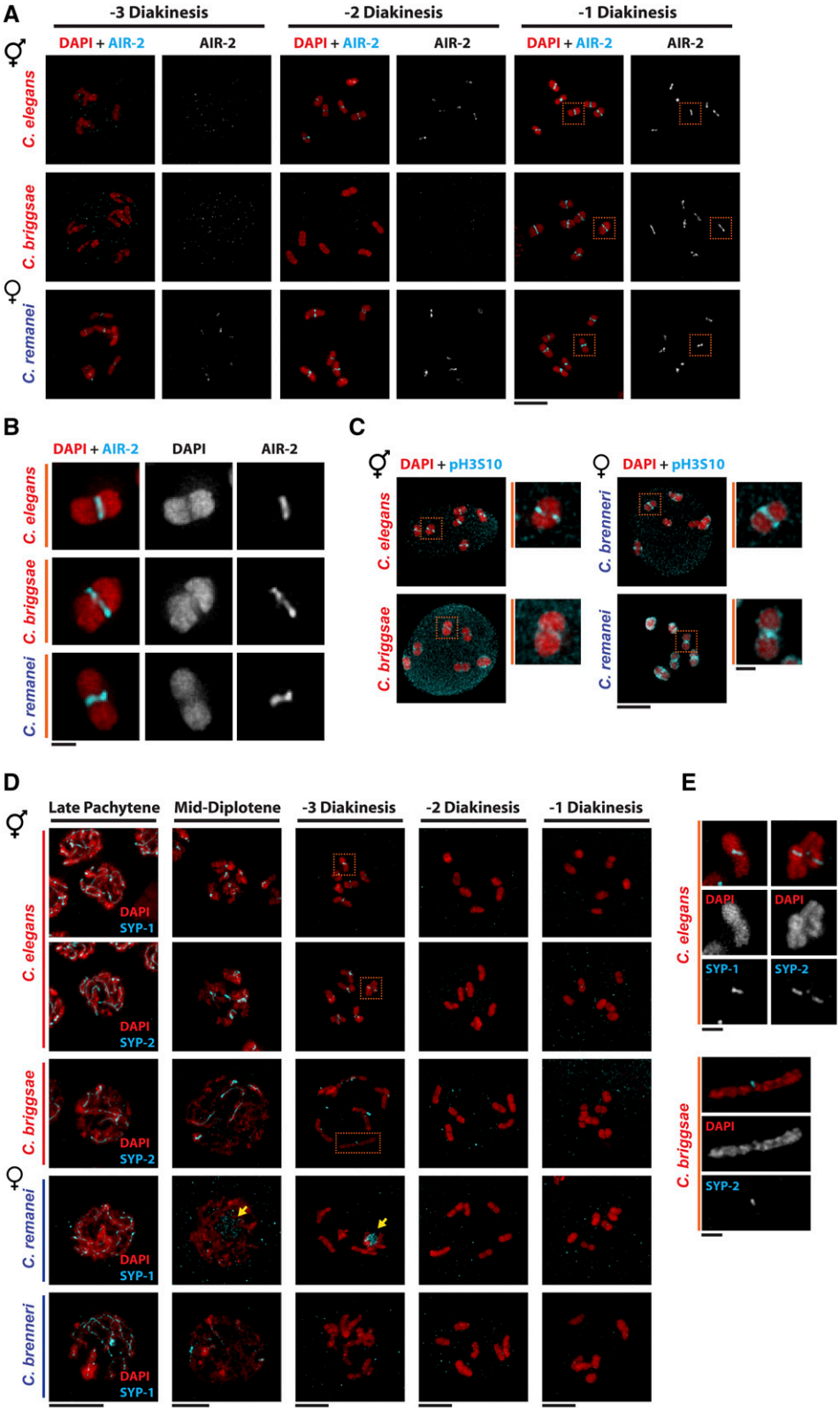

Figure 2 Conservation of bivalent restructuring suggests a single crossover is formed per chromosome pair in *Caenorhabditis*. (A) Immunolocalization of AIR-2 (cyan) in *C. elegans*, *C. briggsae*, and *C. remanei* female/hermaphrodite at −3, −2, and −1 position of diakinesis (see Figure 1A). *C. brenneri* diakinesis nuclei were omitted as no specific staining was observed with the *Cel*-AIR-2 antibody. The various positions (−3, −2, and −1) of diakinesis indicate its position relative to the spermatheca, with the oocyte in the −1 position being the most mature and closest to the spermatheca. Bar, 5 μM. (B) A blow-up of a single −1 diakinesis-stage bivalent for *C. elegans*, *C. briggsae*, and *C. remanei*. Bar, 1 μM. (C) Immunolocalization of pH3S10 (cyan) in *C. elegans*, *C. briggsae*, *C. remanei*, *and C. brenneri* female/hermaphrodite at −1 position of diakinesis with a blow-up of a single bivalent. (D) LP, mid-diplotene, and −3 to −1 position diakinesis nuclei stained with DAPI (red) and either anti-SYP-2 (cyan) for *C. elegans* and *C. briggsae* or anti-SYP-1 (cyan) for *C. remanei* and *C. brenneri*. Yellow arrows point to SYP polycomplex. Bar, 5 μM. (E) A blow-up of a single −3 diakinesis-stage bivalent for *C. elegans* and *C. briggsae*. Bar, 1 μM.

recombination landscape (Reinke *et al.* 2000; Reuben and Lin 2002; Bean *et al.* 2004; Rockman and Kruglyak 2009; Jaramillo-Lambert and Engebrecht 2010; Checchi *et al.* 2014). Although there are different repressive chromatin marks enriched on X chromosomes in these different *Caenorhabditis* species, in all cases, they are devoid of the active mark histone 3 lysine 4 dimethylation (H3K4me2) (Larson *et al.* 2016). To specifically monitor DSB repair on X chromosomes,

we costained germ lines with antibodies recognizing RAD-51 and H3K4me2. RAD-51 was clearly present on the X chromosome pair during oogenesis in all *Caenorhabditis* species, ranging from 8 to 25% of total RAD-51 foci at pachytene (Figure 3). If DSBs as marked by RAD-51 were evenly distributed at pachytene between all chromosome pairs, which are relatively equal in size (Hillier *et al.* 2007), we would expect the same number of RAD-51 foci on the X chromosome pair as on an autosome pair (X RAD-51 foci to autosome RAD-51 ratio of 1). In hermaphrodite/female germ cells, we observed ratios of 1.09 (*C. elegans*), 1.67 (*C. briggsae*), 0.43 (*C. remanei*), and 0.67 (*C. brenneri*), suggesting that DSBs are not evenly distributed. In particular, significantly fewer RAD-51 foci are on the X compared to the autosomes at pachytene in the female/male species (Figure 3A, Figure S5A, and Figure S6B). These differences could reflect differences in distribution, timing of break formation, and/or kinetics of repair and may be influenced by the heterochromatin-like state of the X as previously suggested for *C. elegans* (Gao *et al.* 2015).

We observed a more extreme situation in male germ cells, with significantly fewer RAD-51 foci on the single X chromosome of males in the female/male species compared to the hermaphrodite/male species (Figure 3, B and C and Figure S5B). Twenty-one percent and 14% of RAD-51 foci were observed on the X chromosome of males at pachytene in *C. elegans* and *C. briggsae*, respectively. On the other hand, 0.6 and 1% of RAD-51 foci were observed on the single X in *C. remanei* and *C. brenneri* male pachytene germ cells, respectively (Figure 3B). The X:A ratios were 2.38 (*C. elegans*), 1.67 (*C. briggsae*), 0.06 (*C. remanei*), and 0.10 (*C. brenneri*). These ratios are per chromosome to account for the single X chromosome *vs.* the two chromosomes per autosome pair and are significantly different between the androdioecious *vs.* gonochoristic species (Figure S6A). The differences are likely a consequence of both the higher numbers of RAD-51 on the autosomes and the reduced numbers of RAD-51 on the X chromosome. Indeed, the average number of RAD-51 on the X were also significantly lower in the female/male *vs.* hermaphroditic species (Figure S5 and Figure S6). Further, the X:A ratios and average RAD-51 on the X chromosome(s) of the males *vs.* the hermaphrodites/females were highly statistically different in the gonochoristic species (Figure S6C). In the female/male *C. nigoni*, we also observed very few breaks on the X (Figure 3D, 0.43% of RAD-51 on X). In the hermaphroditic/male species *C. tropicalis*, we saw low but detectable levels of RAD-51 on the X chromosome of males, which was statistically different from both the other hermaphrodite/male species and the female/male species (*C. tropicalis vs. C. remanei*, *C. brenneri*, *C. nigoini*, $P < 0.05$; *C. tropicalis vs. C. elegans*, *C. briggsae*, $P < 0.0001$, Student's *t*-test; Figure 3D). Nonetheless, although overall levels of RAD-51 are higher in gonochoristic species, many fewer RAD-51 foci are detected on the X, suggesting that the X chromosome is not a good substrate for the meiotic DSB machinery in *C. remanei* and *C. brenneri*.

X chromosome pseudosynapsis and DNA repair pathway choice

We previously reported that the single X chromosome of *C. elegans* male germ cells undergoes transient pseudosynapsis early in prophase and has increased flexibility of DSB repair pathway choice compared to autosomes (Checchi *et al.* 2014). We proposed that these alterations allow for accommodation of hemizygosity. Our analysis of RAD-51 loading and disassembly on X chromosomes above suggested that there could be alternative strategies for dealing with hemizygosity in these related species. To determine whether the X chromosome of males in these other species also underwent pseudosynapsis, we stained male germ lines with antibodies directed against SC central region components, SYP-1 or SYP-2 (MacQueen *et al.* 2002; Colaiácovo *et al.* 2003), which we previously reported recognize the corresponding SYPs in these species but is not present on the X chromosome in pachytene nuclei (Larson *et al.* 2016).

In *C. elegans*, transient SYP loading on the X chromosome of males occurs in the TZ where chromosomes are not well separated and acquisition of X-specific chromatin marks is being established. Consequently, the X chromosome can only be unambiguously identified in a subset of TZ nuclei by absence of H3K4me2. Consistent with our previous analysis of SYP-1 (Checchi *et al.* 2014), 9.4% of TZ nuclei where the X could be identified contained SYP-2 on the X chromosome of *C. elegans* males (Figure 4). In contrast to *C. elegans*, we detected no SYP-1 on the X in *C. remanei* and *C. brenneri* in those TZ nuclei where the X could be identified (Figure 4, of >100 nuclei scored). On the other hand, while the majority of *C. briggsae* male TZ germ cells contained no SYP-2 staining on the X chromosome, 3.7% of TZ nuclei where the X could be identified contained SYP-2. These findings suggest that the X chromosome of *C. elegans* and *C. briggsae* male germ cells undergoes transient pseudosynapsis and loads RAD-51 at meiotic DSBs, while neither pseudosynapsis nor RAD-51 foci are observed on the X chromosomes of *C. remanei* and *C. brenneri* male germ cells.

We next addressed whether repair of X-specific breaks can proceed when HR is blocked in *C. briggsae* male germ cells as in *C. elegans*. To that end, we depleted *Cbr*-RAD-54 using the *C. briggsae* strain susceptible to RNAi by feeding (Nuez and Felix 2012). RAD-54 is essential for RAD-51-mediated strand exchange during HR and is required for RAD-51 disassembly (Solinger *et al.* 2002; Mets and Meyer 2009); consequently, inactivation of RAD-54 results in high levels of RAD-51 because DSBs cannot be repaired by HR, remain loaded with RAD-51, and signal for additional break formation because a crossover cannot be formed (Rosu *et al.* 2013; Stamper *et al.* 2013). To test the efficiency of RNAi, we monitored progeny viability in worms propagated on RNAi medium for two generations and observed greatly increased inviability in the presence of *Cbr*-RAD-54 dsRNA [*Cbr*-WT (L4440 control): 2.7 ± 0.8% *vs.* *Cbr-rad-54*(RNAi): 95.3 ± 1.7% inviable

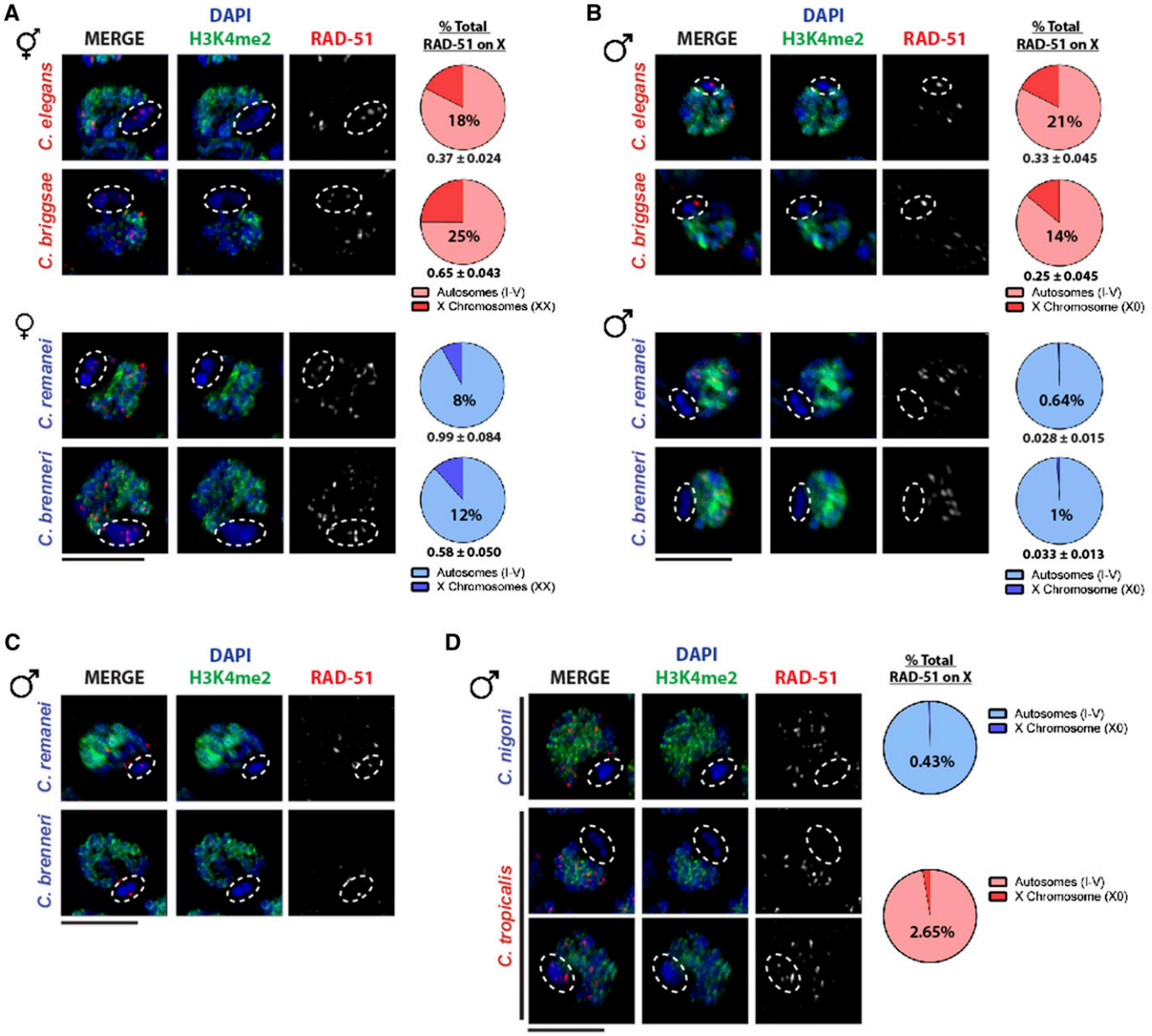

Figure 3 X-specific RAD-51 in *Caenorhabditis* germ cells. (A and B) *C. elegans*, *C. briggsae*, *C. remanei*, and *C. brenneri* female/hermaphrodite and male EP to MP nuclei stained with DAPI (blue), anti-H3K4me2 (green), and anti-RAD-51 (red). White dashed circles denote the X chromosome(s) identified by absence of H3K4me2. Pie graphs comparing percentage of total RAD-51 found on the X chromosome(s) for each species. Below the pie graphs is the average number of RAD-51 on the X chromosome(s) with the standard error of mean. A minimum of three germ lines were examined for each species. (C) A rare *C. remanei* and *C. brenneri* nuclei with RAD-51 localized to the male X chromosome. (D) *C. nigoni* and *C. tropicalis* male pachytene nuclei stained with DAPI (blue), anti-H3K4me2 (green), and RAD-51 (red). White dashed circles denote the X chromosome identified by absence of H3K4me2. Pie graphs comparing percentage of total RAD-51 found on the X chromosome for each species. All bars, 5 μM.

progeny, $P < 0.0001$], consistent with efficient knockdown of *Cbr*-RAD-54.

As the RNAi feeding strain has two genomic regions that lack H3K4me2, the X chromosome and the integrated *Cel-sid-2* array on chromosome V, we monitored X-specific RAD-51 foci by costaining with SYP-2, which is not on the X in pachytene germ cells (Larson *et al.* 2016). Analysis of RAD-51 foci in *Cbr-rad-54*(RNAi) worms revealed high levels of RAD-51 foci genomewide (Figure 5, A and B); however, there was only a modest increase of X-specific RAD-51 foci in mid–late pachytene (Figure 5, A and C). While this data suggests that *Cbr*-RAD-54 contributes to repair of X-specific breaks, it is likely that RAD-51 was disassembled on at least a subset of X DSBs in the absence of *Cbr*-RAD-54, as a significantly smaller percentage of the total RAD-51 foci localized to the X during pachytene [Figure 5D, 1.5% in *Cbr-rad-54*(RNAi) *vs.* 14% in wild-type males, $P < 0.001$, Pearson's χ^2 test]. Thus similar to *C. elegans*, meiotic DSBs on the X chromosome can be repaired in the absence of RAD-54 in *C. briggsae* male germ cells.

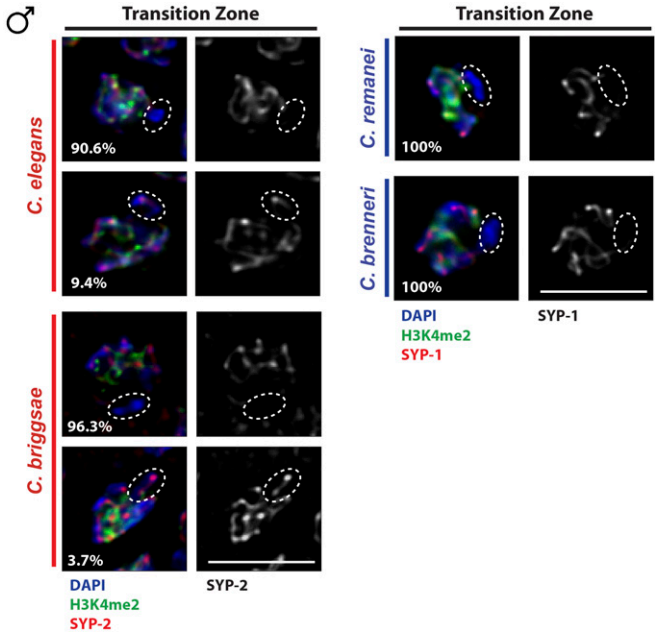

Figure 4 Transient pseudosynapsis of the X chromosome in *C. elegans* and *C. briggsae* male germ cells . TZ nuclei stained with DAPI (blue), H3K4me2 (green), and either anti-SYP-2 (red) for *C. elegans* and *C. briggsae* or anti-SYP-1 (red) for *C. remanei* and *C. brenneri*. White dashed circles denote the single X chromosome of males based on the absence of H3K4me2 staining. Number of TZ nuclei examined from a minimum of six germ lines. *C. elegans*, 149; *C. briggsae*, 107; *C. remanei*, 116; and *C. brenneri*, 125. Bar, 5 μM.

The X chromosome of C. remanei and C. brenneri males is not a substrate of the DSB formation machinery

In contrast to *C. elegans* and *C. briggsae*, very few RAD-51 foci were observed on the X chromosome of *C. remanei* and *C. brenneri* male germ cells (Figure 3, <1%). Because the X chromosome is enriched for heterochromatin marks and highly compacted, antibody accessibility could be an issue, even though antibodies directed against heterochromatin marks are readily detected on the X in male germ cells in these species (Larson *et al.* 2016). Alternatively, the X chromosome may not be subject to SPO-11-dependent breaks. To distinguish between these possibilities, we treated worms with γ-IR to induce DNA breaks; in the *C. elegans* germ line, IR-induced breaks are loaded with RAD-51 (Polanowska *et al.* 2006; Hayashi *et al.* 2007). We exposed worms to 10 Gy of IR, which in *C. elegans* results in ∼3.9 breaks/chromosome pair (Yokoo *et al.* 2012), thus we would predict fewer than two breaks on the single X chromosome of males. We dissected germ lines 30 min following IR exposure and stained extruded germ lines with RAD-51 antibodies. We saw a significant increase in RAD-51 foci on the X at all stages of meiotic prophase in both *C. remanei* and *C. brenneri* (Figure 6, A and B, −IR *vs.* +IR, $P < 0.001$, *t*-test). In both species, there were more RAD-51 foci on the X in EP compared to LP (average RAD-51 foci on X: *C. remanei*, EP: 0.9 ± 0.11; MP: 0.64 ± 0.10; LP: 0.37 ± 0.07; *C. brenneri*, EP: 1.53 ± 0.16; MP: 1.51 ± 0.19; LP: 1.24 ± 0.16). The change in number of RAD-51 foci throughout pachytene may reflect the engagement of different repair pathways late in prophase, as has been observed in *C. elegans* (Hayashi *et al.* 2007; Smolikov *et al.* 2007a). Additionally, the difference in the number of breaks between *C. remanei* and *C. brenneri* may be a consequence of differences in the kinetics of repair of IR-induced breaks. Thus, these results indicate that breaks loaded with RAD-51 on the X chromosome of *C. remanei* and *C. brenneri* can be detected by antibody staining and suggest that meiotic breaks are not induced on the X. Alternatively, it is possible that meiotic DSBs are induced but are not resected to load RAD-51, which is unlikely, given that RAD-51 is loaded on IR-induced breaks (Figure 6).

We also examined RAD-51 foci on the X chromosome over time following exposure to 10 Gy of IR in *C. remanei* male germ cells (Figure S7). Consistent with the analysis above, RAD-51 was readily detected on the X chromosome after 30 min, levels increased slightly at 2 hr following IR, and then slowly decreased at 4 and 8 hr following IR treatment. These results suggest that it takes significant time to process IR-induced breaks.

In addition to being highly compacted, the X chromosome tends to reside in a separate domain from the bulk of the autosomes and we noted that both the compaction state and relationship to the autosomes appeared altered upon IR treatment (Figure 6C). Consistent with a change in compaction, X chromosomes loaded with RAD-51 following IR contained low levels of the activating mark, H3K4me2 (Figure 6C). To explore the spatial configuration of the X in more detail, we costained extruded germ lines isolated from worms before and after IR treatment with an antibody that recognizes the nuclear pore complex (NPC), SYP-1 to identify the X, and RAD-51 (Figure 6D). In the absence of IR, the X chromosome was very compact and was in close proximity to the nuclear envelope in such a manner as to exclude NPCs (Figure 6D, −IR). Upon IR treatment, the X chromatin appeared much more diffuse and was in the same domain as the autosomes. Additionally, the X appeared to have moved inward such that NPCs were no longer excluded from the region adjacent to the X chromosome. Thus, in response to IR, the X chromosome is altered both in terms of chromatin state and nuclear position, presumably to accommodate break repair.

Discussion

Here we show that while many aspects of meiosis are conserved, there are a number of differences in the meiotic process among *Caenorhabditis* species. Strikingly, we discovered that these different species have adopted distinct strategies to accommodate the hemizygous X chromosome during male meiosis. These results suggest that in addition to sex chromosomes having evolved independently in multiple lineages, molecular pathways promoting transmission of hemizygous sex chromosomes through meiosis have diverged substantially even within the same lineage.

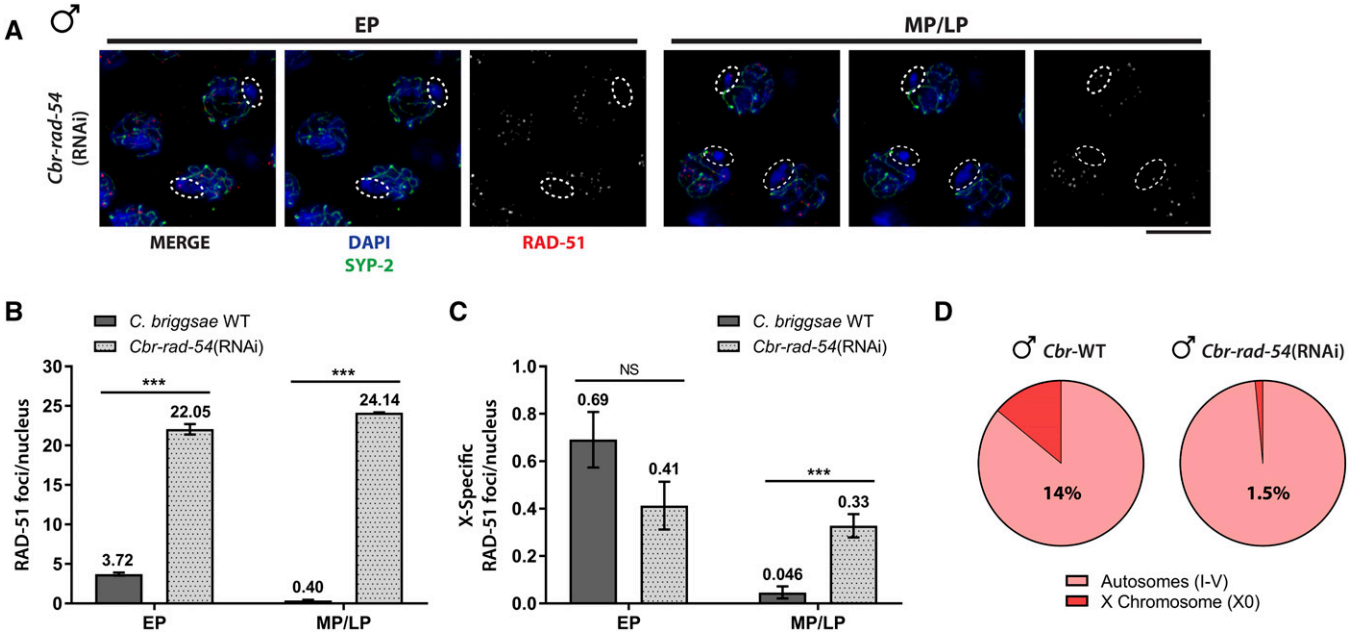

Figure 5 RAD-51 disassembly on the *C. briggsae* male X chromosome in the absence of RAD-54. (A) EP and MP/LP nuclei stained with DAPI (blue), anti-SYP-2 (green), and anti-RAD-51 (red). White dashed circles denote the X chromosome identified by absence of SYP-2. Bar, 5 μM. (B and C) Comparison of total genomewide RAD-51 and RAD-51 on the X chromosome from *C. briggsae* wild-type and *C. briggsae* worms treated with *cbr-rad-54*(RNAi). Error bars = SEM. NS, nonsignificant; *** $P < 0.0001$, Student's *t*-test. (D) Pie graph with the percentage of total RAD-51 found on the X chromosome during pachytene in *C. briggsae* wild-type and *cbr-rad-54*(RNAi) males.

DSB levels vary considerably between Caenorhabditis species

We previously showed that the overall meiotic program is similar between *Caenorhabditis* species (Larson *et al.* 2016). Using RAD-51 foci as an indirect readout of DSB formation and repair, we show here that there appears to be substantially more meiotic DSBs in *C. remanei* and *C. brenneri*, compared to *C. elegans* and *C. briggsae*. Differences in repair kinetics are also likely to contribute to the numbers of RAD-51 observed. The difference in RAD-51 foci between female/male *vs.* hermaphrodite/male species is not merely a consequence of the decrease in genome size attributed to hermaphroditism (Fierst *et al.* 2015), as we observe two to three times the number of RAD-51 foci in *C. remanei* and *C. brenneri*, which have only ∼30% larger genomes compared to *C. elegans* and *C. briggsae*. Environmental differences, particularly temperature, have also been shown to influence recombination (Bomblies *et al.* 2015), suggesting that the differences in DSBs could be a consequence of these species' ecology. However, the *Caenorhabditis* species examined here have been shown to cohabitate and are relatively cosmopolitan in their distribution, except *C. brenneri*, which is restricted to tropical zones (Kiontke *et al.* 2011). Thus, there is no simple correlation with either genome size or habitat that explains the difference in level of DSBs. Could these differences be a consequence of the different reproductive lifestyles of these nematodes? Perhaps hermaphroditic selfing selects against high numbers of DSBs, as DSBs are unlikely to generate genetic variation and only a single crossover is formed per chromosome pair. Consistent with this, analysis of gonochoristic *C. nigoni*, a sister species of *C. briggsae* that can produce fertile interspecies offspring with *C. briggsae* (Woodruff *et al.* 2010; Kiontke *et al.* 2011), also shows high levels of RAD-51 foci, while the other hermaphrodite/male species within the *elegans* group, *C. tropicalis*, shows low levels (Figure 1H). Thus, among the species examined here, reproductive mode appears to correlate with meiotic DSB levels.

DSBs are not evenly distributed along the genome, but tend to be enriched at hotspots. Recent genomic analyses across *Saccharomyces* yeast species revealed a remarkable level of conservation of both the strength and position of DSB hotspots (Lam and Keeney 2015). In this taxa, DSBs are targeted to promoters suggesting that the conservation of hotspots reflects chromosomal feature (*i.e.*, promoters) that are under evolutionary constraint. A similar conservation of hotspots has also been reported in birds (Singhal *et al.* 2015). These results contrast with the remarkable level of divergence of DSB hotspots in mammals, which rely on the zinc finger histone H3K4 methylase, PRDM9 (reviewed in de Massy 2013). As in yeast and birds, *Caenorhabditis* does not have a PRDM9 ortholog; however, recombination mapping and preliminary RAD-51 chromatin immunoprecipitation analyses in *C. elegans* suggest that there are no hotspots *per se*, although RAD-51 is enriched at actively transcribing genes (Rockman and Kruglyak 2009; Kaur and Rockman 2014; Yu *et al.* 2016). The absence of hotspots may allow for flexibility in the levels, and perhaps position, of DSBs in these different species.

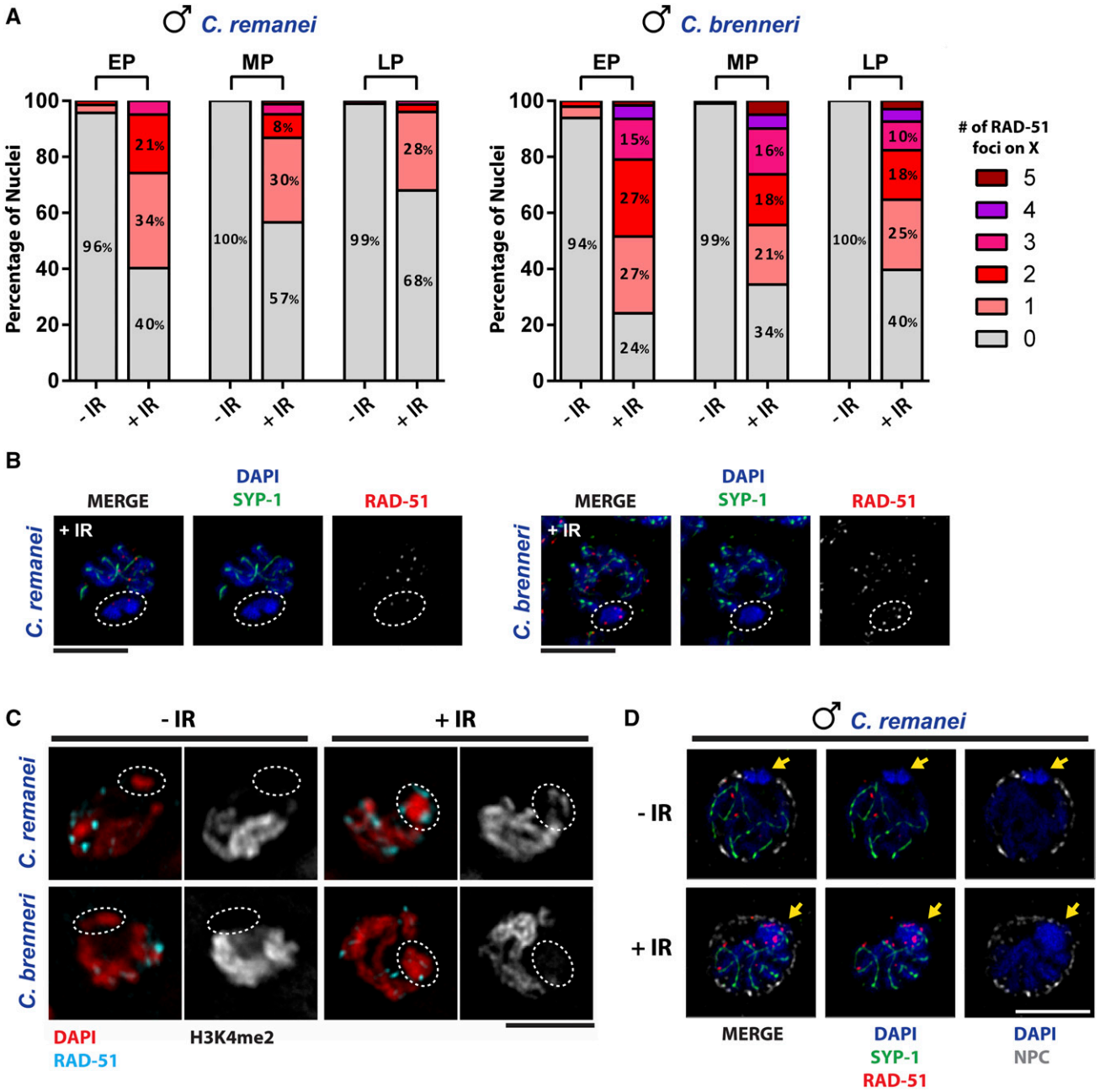

Figure 6 IR-induced breaks load RAD-51 on the X chromosome of *C. remanei* and *C. brenneri* male germ cells. (A) Graph showing the percentage of nuclei with 0–5 RAD-51 foci on the X chromosome of *C. remanei* and *C. brenneri* male germ cells before and after IR at EP, MP, and LP. Worms were treated with 10 Gy of IR and allowed to recover for 30 min. A minimum of 60 nuclei were examined for each species and condition. (B) Pachytene nuclei stained with DAPI (blue), anti-SYP-1 (green), and anti-RAD-51 (red) in *C. remanei* and *C. brenneri* males treated with 10 Gy of IR and allowed to recover for 30 min. White dashed circles denote the single X chromosome of males based on the absence of SYP-1 staining. (C) Pachytene nuclei stained with DAPI (red), anti-RAD-51 (cyan), and H3K4me2 (gray) in *C. remanei* and *C. brenneri* male germ cells before and after IR. White dashed circles denote the single X chromosome of males based on the absence or partial absence of H3K4me2 staining. (D) Pachytene nuclei stained with DAPI (blue), anti-RAD-51 (red), anti-SYP-1 (green), and NPC (gray) in *C. remanei* males before and after IR. Image is a single slice through the middle of the nucleus. Yellow arrows mark the single X chromosome of male germ cells based on the absence of SYP staining. All bars, 5 μM.

Ultimately, DSBs will need to be mapped at the molecular level to determine what chromosomal features facilitate DSB formation in *Caenorhabditis*, and whether this is altered between species. There is precedence for differences in recombination between species in the same genus as illustrated in *Drosophila* where *D. melanogaster* males do not exhibit any meiotic recombination, while some populations of *D. ananassae* do (Goni *et al.* 2016). Further, recombination can vary widely between the sexes, and even within individuals of the same species (Fledel-Alon *et al.* 2011).

Single crossover per chromosome pair as an adaptation to holocentry

In all species examined, many more DSBs are induced than will be processed into crossovers (Lake and Hawley 2016). In some species, this reflects the role of DSB repair in the process of chromosome pairing (reviewed in Zickler and Kleckner 2015). However, in *C. elegans* and *Drosophila*, where chromosome pairing can occur in the absence of meiotic recombination (Dernburg *et al.* 1998; McKim and Hayashi-Hagihara 1998), there are still more DSBs than crossovers (Colaiácovo *et al.* 2003; Mehrotra and McKim 2006). The relationship between DSBs and crossovers is complex, as enough DSBs must be induced to ensure that every chromosome receives a crossover for disjunction. Conversely, excess crossovers are deleterious and are inhibited by the process of crossover interference (reviewed in Zickler and Kleckner 2016). *C. elegans* represents an extreme case of crossover interference as on average only a single crossover is formed per chromosome pair (Meneely *et al.* 2002; Hillers and Villeneuve 2003). We provide evidence that strong crossover interference is likely a conserved feature of *Caenorhabditis* and is perhaps even more potent in those species with more DSBs. We propose that limiting crossovers to one per chromosome pair is an adaptation to holocentry in *Caenorhabditis*. Beautiful work in *C. elegans* has shown that the single crossover per chromosome pair in meiosis is essential for the restructuring of the bivalent into a long and short arm (Nabeshima *et al.* 2005). Restructured bivalents allow for regulated cohesin release on the short arms, and in combination with kinetochores forming a cup-like structure around the long arm ends, ensure proper chromosome segregation during meiosis (de Carvalho *et al.* 2008; Dumont *et al.* 2010). Although restructuring of the bivalent is conserved among *Caenorhabditis* (Figure 2), the details are different between the species. In particular, disassembly of SC central region components has a distinct pattern in each species. Whether this is a consequence of differences in the number of diplotene/diakinesis nuclei (Larson *et al.*, 2016), or an inherent difference in how the SC is disassembled, is not known.

Consistent with formation of a single crossover per chromosome pair, in *C. elegans* each chromosome has a genetic length of ~50 cM. Genomic analyses and recombinant inbred lines have been used to generate a genetic map for *C. briggsae*, which are also consistent with formation of a single crossover per chromosome (Hillier *et al.* 2007; Ross *et al.* 2011). Additionally, several chromosomal features, such as less recombination in the center compared to the arms, suggest that the crossover landscape is similar between these species. Much more limited analysis has been performed on *C. remanei* and *C. brenneri*, but it is likely that they are also limited to a single crossover per chromosome arm to ensure disjunction, consistent with our analysis of bivalent restructuring.

Different strategies to accommodate sex chromosome hemizygosity

Remarkably, we show that species within the *Caenorhabditis* genus use very different strategies to accommodate sex chromosome hemizygosity, even though the emergence of sex chromosomes likely predated the *Caenorhabditis* lineage. The single X chromosome of males in both *C. elegans* and *C. briggsae* germ cells undergoes a transient period of pseudosynapsis contemporaneous with DSB formation (Checchi *et al.* 2014) (Figure 4). Further, in both species, break repair can precede in the absence of HR (Checchi *et al.* 2014) (Figure 5). Thus, in *C. elegans* and *C. briggsae* we propose that hemizygosity is accommodated by the X sister chromatids masquerading as an autosome pair early in meiosis and as meiosis proceeds, the constraints on DSB repair are relaxed. In *C. tropicalis*, the other independently derived hermaphrodite/male species, we observed significantly fewer breaks on the X than *C. elegans* or *C. briggsae*, but more than in the female/male species. Perhaps *C. tropicalis* represents an intermediate state between *C. elegans* and *C. briggsae vs.* the female/male species. The predicted phylogeny of the *elegans* group suggests that *C. tropicalis* diverged from its gonochoristic ancestor longer ago than *C. briggsae* (Kiontke *et al.* 2011). Thus it is equally likely that *C. tropicalis* uses a different strategy to accommodate sex chromosome hemizygosity than either the other hermaphroditic species or the three gonochoristic species we examined here.

The lack of DSBs, as marked by RAD-51, on the *C. remanei* and *C. brenneri* (and *C. nigoni*) X chromosome of males suggests that SPO-11 can be prevented from breaking a chromosome, which would be advantageous when a homologous chromosome is not present as a template for repair. While we show that SYP-1 is not loaded onto these chromosomes, it remains to be determined whether axial components are loaded onto the X as they are in *C. elegans* (Jaramillo-Lambert and Engebrecht 2010), and we presume in *C. briggsae*. Of particular interest would be to assess whether the HORMA domain protein, HTP-3, which is essential for DSB formation (Goodyer *et al.* 2008), is present on the X chromosome of *C. remanei* and *C. brenneri*. If HTP-3 is not loaded on the X, this would provide an explanation for why SPO-11 does not induce breaks. However, as HTP-3 is loaded very early during meiosis prior to chromosome pairing, it would be surprising if HTP-3 was not loaded on the X. Unfortunately, axial components are not well conserved and therefore we were unable to examine HTP-3 in these other species.

One feature of sex chromosomes that is likely to influence breakage and repair is their repressive chromatin nature. It is well documented that repair kinetics and repair pathway choice are distinct in euchromatin *vs.* heterochromatin (Xu and Price 2011). Further, previous analysis indicated that the X chromosome pair in *C. elegans* hermaphroditic germ cells had fewer DSBs than the autosomes as a consequence of the unique chromatin landscape of the X (Gao *et al.* 2015). However, although enriched for repressive chromatin marks, the X is not a classic heterochromatin domain with repetitive sequences. Further, it is unlikely that a single repressive mark dictates either the extent of breakage or mode of repair, as the X chromosome of *C. elegans* (RAD-51^{+}) and *C. remanei* (RAD-51^{-}) is enriched for H3K9me2 while the X chromosome

of *C. briggsae* (RAD-51$^+$) and *C. brenneri* (RAD-51$^-$) is enriched for H3K9me3 (Larson *et al.* 2016). Consistent with this, inactivation of MET-2, a SETBD1 histone methyltransferase responsible for acquisition of these repressive chromatin marks, does not alter meiotic DSB levels in *C. elegans* (Checchi and Engebrecht 2011), although MET-2 may influence DSB distribution (Yu *et al.* 2016).

Recent work in both *Drosophila* and mammalian tissue culture has shown that DSBs within heterochromatin domains move outside of the heterochromatic region for repair by HR (Chiolo *et al.* 2011; Ryu *et al.* 2015; Tsouroula *et al.* 2016). In both of these systems, HR occurs at the nuclear periphery. We provide evidence that the X chromosome of *C. remanei* and *C. brenneri* male germ cells is sequestered at the nuclear periphery where we propose SPO-11 and associated proteins do not have access. Our analysis of IR-induced breaks in *C. remanei* and *C. brenneri* suggest that the X chromosome also undergoes movement in response to DNA breaks (Figure 6); however, in contrast to what is observed in *Drosophila* and mammals, the X chromosome appears to move away from the nuclear periphery. An important distinction is that we are examining meiotic cells where recombination is actively engaged *vs.* somatic cells, where DSBs are rarely purposefully inflicted on the genome. Further, chromosomes have distinct configurations in meiosis compared to somatic cells, perhaps altering the relationship to the nuclear periphery. Nonetheless, in all of these examples, movement is accompanied by a change in chromatin state. Thus, although there are parallels between the behavior of the X of *C. remanei* and *C. brenneri* males and these classic heterochromatin domains, there are also differences. Whether this reflects genome size and complexity or unique aspects of meiotic cells generally, or sex chromosomes specifically, is not currently known.

Acknowledgments

We thank Jill Shumacher (University of Texas), Sarit Smolikove (University of Iowa), and Anne Villeneuve (Stanford University) for AIR-2, SYP-1/-2, and RAD-51 antibodies, respectively; Katherine Lawrence for discussions; Qianyan Li for help with imaging; and Ryan Jensen for construction of RNAi feeding clones. Some strains were provided by the *Caenorhabditis* Genetics Center, which is funded by the National Institutes of Health (NIH) Office of Research Infrastructure Programs (P40-OD010440). This work was supported by NIH grant GM-103860 and the Agricultural Experimental Station California-Davis grant *MCB-7237-H (to J.E.).

Literature Cited

Albertson, D. G., A. M. Rose, and A. M. Villeneuve, 1997 Chromosome organization, mitosis, and meiosis, in *C. elegans II*, edited by D. L. Riddle, T. Blumenthal, B. J. Meyer, and J. R. Priess, Cold Spring Harbor Laboratory Press, Cold Spring Harbor, NY.

Alpi, A., P. Pasierbek, A. Gartner, and J. Loidl, 2003 Genetic and cytological characterization of the recombination protein RAD-51 in *Caenorhabditis elegans*. Chromosoma 112: 6–16.

Bean, C. J., C. E. Schaner, and W. G. Kelly, 2004 Meiotic pairing and imprinted X chromatin assembly in *Caenorhabditis elegans*. Nat. Genet. 36: 100–105.

Bishop, D. K., D. Park, L. Xu, and N. Kleckner, 1992 DMC1: a meiosis-specific yeast homolog of E. coli recA required for recombination, synaptonemal complex formation, and cell cycle progression. Cell 69: 439–456.

Bomblies, K., J. D. Higgins, and L. Yant, 2015 Meiosis evolves: adaptation to external and internal environments. New Phytol. 208: 306–323.

Brown, M. S., and D. K. Bishop, 2015 DNA strand exchange and RecA homologs in meiosis. Cold Spring Harb. Perspect. Biol. 7: a016659.

Checchi, P. M., and J. Engebrecht, 2011 *Caenorhabditis elegans* histone methyltransferase MET-2 shields the male X chromosome from checkpoint machinery and mediates meiotic sex chromosome inactivation. PLoS Genet. 7: e1002267.

Checchi, P. M., K. S. Lawrence, M. V. Van, B. J. Larson, and J. Engebrecht, 2014 Pseudosynapsis and decreased stringency of meiotic repair pathway choice on the hemizygous sex chromosome of *Caenorhabditis elegans* males. Genetics 197: 543–560.

Chiolo, I., A. Minoda, S. U. Colmenares, A. Polyzos, S. V. Costes *et al.*, 2011 Double-strand breaks in heterochromatin move outside of a dynamic HP1a domain to complete recombinational repair. Cell 144: 732–744.

Coghlan, A., 2005 Nematode genome evolution. WormBook 1–15.

Colaiácovo, M. P., A. J. MacQueen, E. Martinez-Perez, K. McDonald, A. Adamo *et al.*, 2003 Synaptonemal complex assembly in *C. elegans* is dispensable for loading strand-exchange proteins but critical for proper completion of recombination. Dev. Cell 5: 463–474.

Cole, F., S. Keeney, and M. Jasin, 2010 Evolutionary conservation of meiotic DSB proteins: more than just Spo11. Genes Dev. 24: 1201–1207.

Collette, K. S., E. L. Petty, N. Golenberg, J. N. Bembenek, and G. Csankovszki, 2011 Different roles for Aurora B in condensin targeting during mitosis and meiosis. J. Cell Sci. 124: 3684–3694.

de Carvalho, C. E., S. Zaaijer, S. Smolikov, Y. Gu, J. M. Schumacher *et al.*, 2008 LAB-1 antagonizes the Aurora B kinase in *C. elegans*. Genes Dev. 22: 2869–2885.

de Massy, B., 2013 Initiation of meiotic recombination: How and where? Conservation and specificities among eukaryotes. Annu. Rev. Genet. 47: 563–599.

Dernburg, A. F., K. McDonald, G. Moulder, R. Barstead, M. Dresser *et al.*, 1998 Meiotic recombination in *C. elegans* initiates by a conserved mechanism and is dispensable for homologous chromosome synapsis. Cell 94: 387–398.

Dumont, J., K. Oegema, and A. Desai, 2010 A kinetochore-independent mechanism drives anaphase chromosome separation during acentrosomal meiosis. Nat. Cell Biol. 12: 894–901.

Fierst, J. L., J. H. Willis, C. G. Thomas, W. Wang, R. M. Reynolds *et al.*, 2015 Reproductive mode and the evolution of genome size and structure in *Caenorhabditis* nematodes. PLoS Genet. 11: e1005323.

Fledel-Alon, A., E. M. Leffler, Y. Guan, M. Stephens, G. Coop *et al.*, 2011 Variation in human recombination rates and its genetic determinants. PLoS One 6: e20321.

Gao, J., H. M. Kim, A. E. Elia, S. J. Elledge, and M. P. Colaiácovo, 2015 NatB domain-containing CRA-1 antagonizes hydrolase ACER-1 linking acetyl-CoA metabolism to the initiation of recombination during *C. elegans* meiosis. PLoS Genet. 11: e1005029.

Garcia, V., S. E. Phelps, S. Gray, and M. J. Neale, 2011 Bidirectional resection of DNA double-strand breaks by Mre11 and Exo1. Nature 479: 241–244.

Goni, B., M. Matsuda, and Y. N. Tobari, 2016 Male recombination in Brazilian populations of *Drosophila ananassae*. Genome 59: 493–500.

Goodyer, W., S. Kaitna, F. Couteau, J. D. Ward, S. J. Boulton *et al.*, 2008 HTP-3 links DSB formation with homolog pairing and crossing over during *C. elegans* meiosis. Dev. Cell 14: 263–274.

Hammarlund, M., M. W. Davis, H. Nguyen, D. Dayton, and E. M. Jorgensen, 2005 Heterozygous insertions alter crossover distribution but allow crossover interference in *Caenorhabditis elegans*. Genetics 171: 1047–1056.

Hayashi, M., G. M. Chin, and A. M. Villeneuve, 2007 *C. elegans* germ cells switch between distinct modes of double-strand break repair during meiotic prophase progression. PLoS Genet. 3: e191.

Hillers, K. J., and A. M. Villeneuve, 2003 Chromosome-wide control of meiotic crossing over in *C. elegans*. Curr. Biol. 13: 1641–1647.

Hillier, L. W., R. D. Miller, S. E. Baird, A. Chinwalla, L. A. Fulton *et al.*, 2007 Comparison of *C. elegans* and *C. briggsae* genome sequences reveals extensive conservation of chromosome organization and synteny. PLoS Biol. 5: e167.

Hsu, J. Y., Z. W. Sun, X. Li, M. Reuben, K. Tatchell *et al.*, 2000 Mitotic phosphorylation of histone H3 is governed by Ipl1/aurora kinase and Glc7/PP1 phosphatase in budding yeast and nematodes. Cell 102: 279–291.

Jaramillo-Lambert, A., M. Ellefson, A. M. Villeneuve, and J. Engebrecht, 2007 Differential timing of S phases, X chromosome replication, and meiotic prophase in the *C. elegans* germ line. Dev. Biol. 308: 206–221.

Jaramillo-Lambert, A., and J. Engebrecht, 2010 A single unpaired and transcriptionally silenced X chromosome locally precludes checkpoint signaling in the *Caenorhabditis elegans* germ line. Genetics 184: 613–628.

Kaitna, S., P. Pasierbek, M. Jantsch, J. Loidl, and M. Glotzer, 2002 The aurora B kinase AIR-2 regulates kinetochores during mitosis and is required for separation of homologous chromosomes during meiosis. Curr. Biol. 12: 798–812.

Kauppi, L., M. Barchi, F. Baudat, P. J. Romanienko, S. Keeney *et al.*, 2011 Distinct properties of the XY pseudoautosomal region crucial for male meiosis. Science 331: 916–920.

Kaur, T., and M. V. Rockman, 2014 Crossover heterogeneity in the absence of hotspots in *Caenorhabditis elegans*. Genetics 196: 137–148.

Keeney, S., C. N. Giroux, and N. Kleckner, 1997 Meiosis-specific DNA double-strand breaks are catalyzed by Spo11, a member of a widely conserved protein family. Cell 88: 375–384.

Kelly, W. G., C. E. Schaner, A. F. Dernburg, M. H. Lee, S. K. Kim *et al.*, 2002 X-chromosome silencing in the germline of *C. elegans*. Development 129: 479–492.

Kiontke, K., and D. H. Fitch, 2005 The phylogenetic relationships of *Caenorhabditis* and other rhabditids. WormBook 1–11.

Kiontke, K. C., M. A. Felix, M. Ailion, M. V. Rockman, C. Braendle *et al.*, 2011 A phylogeny and molecular barcodes for *Caenorhabditis*, with numerous new species from rotting fruits. BMC Evol. Biol. 11: 339.

Lake, C. M., and R. S. Hawley, 2016 Becoming a crossover-competent DSB. Semin. Cell Dev. Biol. 54: 117–125.

Lam, I., and S. Keeney, 2015 Nonparadoxical evolutionary stability of the recombination initiation landscape in yeast. Science 350: 932–937.

Larson, B. J., M. V. Van, T. Nakayama, and J. Engebrecht, 2016 Plasticity in the meiotic epigenetic landscape of sex chromosomes in *Caenorhabditis* species. Genetics 203: 1641–1658.

Lemmens, B. B., N. M. Johnson, and M. Tijsterman, 2013 COM-1 promotes homologous recombination during *Caenorhabditis elegans* meiosis by antagonizing Ku-mediated non-homologous end joining. PLoS Genet. 9: e1003276.

Lui, D. Y., and M. P. Colaiácovo, 2013 Meiotic development in *Caenorhabditis elegans*. Adv. Exp. Med. Biol. 757: 133–170.

MacQueen, A. J., M. P. Colaiácovo, K. McDonald, and A. M. Villeneuve, 2002 Synapsis-dependent and -independent mechanisms stabilize homolog pairing during meiotic prophase in *C. elegans*. Genes Dev. 16: 2428–2442.

McKee, B. D., 1996 The license to pair: identification of meiotic pairing sites in Drosophila. Chromosoma 105: 135–141.

McKim, K. S., and A. Hayashi-Hagihara, 1998 mei-W68 in *Drosophila melanogaster* encodes a Spo11 homolog: evidence that the mechanism for initiating meiotic recombination is conserved. Genes Dev. 12: 2932–2942.

Mehrotra, S., and K. S. McKim, 2006 Temporal analysis of meiotic DNA double-strand break formation and repair in Drosophila females. PLoS Genet. 2: e200.

Meneely, P. M., A. F. Farago, and T. M. Kauffman, 2002 Crossover distribution and high interference for both the X chromosome and an autosome during oogenesis and spermatogenesis in *Caenorhabditis elegans*. Genetics 162: 1169–1177.

Mets, D. G., and B. J. Meyer, 2009 Condensins regulate meiotic DNA break distribution, thus crossover frequency, by controlling chromosome structure. Cell 139: 73–86.

Morelli, M. A., and P. E. Cohen, 2005 Not all germ cells are created equal: aspects of sexual dimorphism in mammalian meiosis. Reproduction 130: 761–781.

Nabeshima, K., A. M. Villeneuve, and M. P. Colaiácovo, 2005 Crossing over is coupled to late meiotic prophase bivalent differentiation through asymmetric disassembly of the SC. J. Cell Biol. 168: 683–689.

Nuez, I., and M. A. Felix, 2012 Evolution of susceptibility to ingested double-stranded RNAs in *Caenorhabditis* nematodes. PLoS One 7: e29811.

Penkner, A., Z. Portik-Dobos, L. Tang, R. Schnabel, M. Novatchkova *et al.*, 2007 A conserved function for a *Caenorhabditis elegans* Com1/Sae2/CtIP protein homolog in meiotic recombination. EMBO J. 26: 5071–5082.

Polanowska, J., J. S. Martin, T. Garcia-Muse, M. I. Petalcorin, and S. J. Boulton, 2006 A conserved pathway to activate BRCA1-dependent ubiquitylation at DNA damage sites. EMBO J. 25: 2178–2188.

Reinke, V., H. E. Smith, J. Nance, J. Wang, C. Van Doren *et al.*, 2000 A global profile of germline gene expression in *C. elegans*. Mol. Cell 6: 605–616.

Reuben, M., and R. Lin, 2002 Germline X chromosomes exhibit contrasting patterns of histone H3 methylation in *Caenorhabditis elegans*. Dev. Biol. 245: 71–82.

Rockman, M. V., and L. Kruglyak, 2009 Recombinational landscape and population genomics of *Caenorhabditis elegans*. PLoS Genet. 5: e1000419.

Rogers, E., J. D. Bishop, J. A. Waddle, J. M. Schumacher, and R. Lin, 2002 The aurora kinase AIR-2 functions in the release of chromosome cohesion in *Caenorhabditis elegans* meiosis. J. Cell Biol. 157: 219–229.

Ross, J. A., D. C. Koboldt, J. E. Staisch, H. M. Chamberlin, B. P. Gupta *et al.*, 2011 *Caenorhabditis briggsae* recombinant inbred line genotypes reveal inter-strain incompatibility and the evolution of recombination. PLoS Genet. 7: e1002174.

Rosu, S., D. E. Libuda, and A. M. Villeneuve, 2011 Robust crossover assurance and regulated interhomolog access maintain meiotic crossover number. Science 334: 1286–1289.

Rosu, S., K. A. Zawadzki, E. L. Stamper, D. E. Libuda, A. L. Reese *et al.*, 2013 The *C. elegans* DSB-2 protein reveals a regulatory network that controls competence for meiotic DSB formation and promotes crossover assurance. PLoS Genet. 9: e1003674.

Ryu, T., B. Spatola, L. Delabaere, K. Bowlin, H. Hopp *et al.*, 2015 Heterochromatic breaks move to the nuclear periphery

to continue recombinational repair. Nat. Cell Biol. 17: 1401–1411.

Shakes, D. C., J. C. Wu, P. L. Sadler, K. Laprade, L. L. Moore *et al.*, 2009 Spermatogenesis-specific features of the meiotic program in *Caenorhabditis elegans*. PLoS Genet. 5: e1000611.

Shinohara, M., S. D. Oh, N. Hunter, and A. Shinohara, 2008 Crossover assurance and crossover interference are distinctly regulated by the ZMM proteins during yeast meiosis. Nat. Genet. 40: 299–309.

Singhal, S., E. M. Leffler, K. Sannareddy, I. Turner, O. Venn *et al.*, 2015 Stable recombination hotspots in birds. Science 350: 928–932.

Smolikov, S., A. Eizinger, A. Hurlburt, E. Rogers, A. M. Villeneuve *et al.*, 2007a Synapsis-defective mutants reveal a correlation between chromosome conformation and the mode of double-strand break repair during *Caenorhabditis elegans* meiosis. Genetics 176: 2027–2033.

Smolikov, S., A. Eizinger, K. Schild-Prufert, A. Hurlburt, K. McDonald *et al.*, 2007b SYP-3 restricts synaptonemal complex assembly to bridge paired chromosome axes during meiosis in *Caenorhabditis elegans*. Genetics 176: 2015–2025.

Smolikov, S., K. Schild-Prufert, and M. P. Colaiácovo, 2009 A yeast two-hybrid screen for SYP-3 interactors identifies SYP-4, a component required for synaptonemal complex assembly and chiasma formation in *Caenorhabditis elegans* meiosis. PLoS Genet. 5: e1000669.

Solinger, J. A., K. Kiianitsa, and W. D. Heyer, 2002 Rad54, a Swi2/Snf2-like recombinational repair protein, disassembles Rad51:dsDNA filaments. Mol. Cell 10: 1175–1188.

Stamper, E. L., S. E. Rodenbusch, S. Rosu, J. Ahringer, A. M. Villeneuve *et al.*, 2013 Identification of DSB-1, a protein required for initiation of meiotic recombination in *Caenorhabditis elegans*, illuminates a crossover assurance checkpoint. PLoS Genet. 9: e1003679.

Timmons, L., D. L. Court, and A. Fire, 2001 Ingestion of bacterially expressed dsRNAs can produce specific and potent genetic interference in *Caenorhabditis elegans*. Gene 263: 103–112.

Tsouroula, K., A. Furst, M. Rogier, V. Heyer, A. Maglott-Roth *et al.*, 2016 Temporal and spatial uncoupling of DNA double strand break repair pathways within mammalian heterochromatin. Mol. Cell 21; 293–305.

Woodruff, G. C., O. Eke, S. E. Baird, M. A. Felix, and E. S. Haag, 2010 Insights into species divergence and the evolution of hermaphroditism from fertile interspecies hybrids of *Caenorhabditis* nematodes. Genetics 186: 997–1012.

Xu, Y., and B. D. Price, 2011 Chromatin dynamics and the repair of DNA double strand breaks. Cell Cycle 10: 261–267.

Yin, Y., and S. Smolikove, 2013 Impaired resection of meiotic double-strand breaks channels repair to nonhomologous end joining in *Caenorhabditis elegans*. Mol. Cell. Biol. 33: 2732–2747.

Yokoo, R., K. A. Zawadzki, K. Nabeshima, M. Drake, S. Arur *et al.*, 2012 COSA-1 reveals robust homeostasis and separable licensing and reinforcement steps governing meiotic crossovers. Cell 149: 75–87.

Yu, Z., Y. Kim, and A. F. Dernburg, 2016 Meiotic recombination and the crossover assurance checkpoint in *Caenorhabditis elegans*. Semin. Cell Dev. Biol. 54: 106–116.

Zedek, F., and P. Bures, 2012 Evidence for centromere drive in the holocentric chromosomes of *Caenorhabditis*. PLoS One 7: e30496.

Zickler, D., and N. Kleckner, 2015 Recombination, Pairing, and Synapsis of Homologs during Meiosis. Cold Spring Harb. Perspect. Biol. **7:** pii a016626.

Zickler, D., and N. Kleckner, 2016 A few of our favorite things: pairing, the bouquet, crossover interference and evolution of meiosis. Semin. Cell Dev. Biol. 54: 135–148.

Communicating editor: M. P. Colaiácovo

A. RAD-51

```
                                                   ↓
Cel-RAD-51      MGQSWGYEGIAKRSLCTHKWLYNLNLHSINLFLPIESKMSAQASRQKKSDQEQRAADQAL
Cbr-RAD-51      --------------------------------------MSAQASRSKKSDQDQRAADQAL
Cre-RAD-51      --------------------------------------MSAQASRQKKTDQDQRAADQAL
Cbn-RAD-51      --------------------------------------MSAQASRQKKTDQEQRAADQAL
                                                       *******.**:**:********

Cel-RAD-51      LN---------------AAIEDNAMEQDENFTVIDKLESSGISSGDISKLKEAGYYTYES
Cbr-RAD-51      LN---------------AAIADNDMEQDENFTVIDKLESTGISSGDISKLKEAGYYTYES
Cre-RAD-51      LNVKQQFSGKYVRKKFQAAIQDNDMEQDENFTIIDKLESTGISSGDISKLKEAGYYTYES
Cbn-RAD-51      LN---------------AAIEDNDMEQDENFTIIDKLESTGISSGDISKLKEAGYYTYES
                **               *** ** ********:******:********************

Cel-RAD-51      LAFTTRRELRNVKGISDQKAEKIMKEAMKFVQMGFTTGAEVHVKRSQLVQIRTGSASLDR
Cbr-RAD-51      LAFTTRRELRNVKGISDQKAEKIMKEAMKYVQMGFTTGAEVHVKRSQLVQIRTGSAALDR
Cre-RAD-51      LAFTTRRELRNVKGISDQKAEKIMKEAMKYVQMGFTTGAEVHVKRSQLVQIRTGSAALDR
Cbn-RAD-51      LAFTTRRELRNVKGISDQKAEKIMKEAMKYVQMGFTTGAEVHVKRSQLVQIRTGSAALDR
                ******************************:***************************:***

Cel-RAD-51      LLGGGIETGSITEVYGEYRTGKTQLCHSLAVLCQLPIDMGGGEGKCMYIDTNATFRPERI
Cbr-RAD-51      LLGGGIETGSITEVYGEYRTGKTQLCHSLAVLCQLPIDMGGGEGKCMYIDTNATFRPERI
Cre-RAD-51      LLGGGIETGSITEVYGEYRTGKTQLCHSLAVLCQLPIDMGGGEGKCMYIDTNATFRPERI
Cbn-RAD-51      LLGGGIETGSITEVYGEYRTGKTQLCHSLAVLCQLPIDMGGGEGKCMYIDTNATFRPERI
                ************************************************************

Cel-RAD-51      IAIAQRYNMDSAHVLENIAVARAYNSEHLMALIIRAGAMMSESRYAVVIVDCATAHFRNE
Cbr-RAD-51      IAIAQRYNMDSAHVLENIAVARAYNSEHLMALIIRAGAMMSESRYAVVIVDCATAHFRNE
Cre-RAD-51      IAIAQRYNMDSAHVLENIAVARAYNSEHLMALIIRAGAMMSESRYAVVIVDCATAHFRNE
Cbn-RAD-51      IAIAQRYNMDSAHVLENIAVARAYNSEHLMALIIRAGAMMSESRYAVVIVDCATAHFRNE
                ************************************************************

Cel-RAD-51      YTGRGDLAERQMKLSAFLKCLAKLADEYGVAVIITNQVVAQVDGGASMFQADAKKPIGGH
Cbr-RAD-51      YTGRGDLAERQMKLSAFLKCLAKLADEYGVAVIITNQVVAQVDGGASMFQADAKKPIGGH
Cre-RAD-51      YTGRGDLAERQMKLSAFLKCLAKLADEYGVAVIITNQVVAQVDGGASMFQADAKKPIGGH
Cbn-RAD-51      YTGRGDLAERQMKLSAFLKCLAKLADEYGVAVIITNQVVAQVDGGASMFQADAKKPIGGH
                ************************************************************

Cel-RAD-51      IIAHMSTT------------------RLYLRKGKGENRVAKMVQSPNLPEAEATYSITNH
Cbr-RAD-51      IIAHMSTT------------------RLYLRKGKGENRVAKMVQSPNLPEAEATYSITNH
Cre-RAD-51      IIAHMSTTRLSVKVIRGHSLTVLFFCRLYLRKGKGENRVAKMVQSPNLPEAEATYSITNH
Cbn-RAD-51      IIAHMSTT------------------RLYLRKGKGENRVAKMVQSPNLPEAEATYSITNH
                ********                  *********************************

Cel-RAD-51      GIEDARED
Cbr-RAD-51      GIEDARED
Cre-RAD-51      GIEDARED
Cbn-RAD-51      GIEDARED
                ********
```

B. AIR-2

```
Cel-AIR-2       MENKPPVINL-PEKETVNTPQKGGKFTINDFEIGRPLGKGKFGSVYLARTKTGHFHVAIK
Cbr-AIR-2       MENKPQILQ----TKSKNTPNKGGKLSINDFEIGRPLGKGKFGSVYLARTKTGHFHCAIK
Cre-AIR-2       MENKPEVIHDHDEKKSKNNPMKGGKLSIKDFEIGRPLGKGKFGSVYLARTKEGHFHCAIK
Cbn-AIR-2       MENKPRVSELA--KKPKYTPDKGGKMSIKDFEIGRPLGKGKFGSVYLARTKTGFFHCAVK
                ***** : .    .:   .* ****::*:********************** *.** *:*

Cel-AIR-2       -------------------------------------------------------VLFKSQL
Cbr-AIR-2       -------------------------------------------------------VLFKSQL
Cre-AIR-2       -------------------------------------------------------VLFKSQL
Cbn-AIR-2       VSLPTGTLSKCALMPWLFWDKIFESARQMNGVQWSALAYADNQLSTVSIPIFQVLFKSQL
                                                                       *******
```

```
Cel-AIR-2      ISGGVEHQLEREIEIQSHLNHPNIIKLYTYFWDAKKIYLVLEYAPGGEMYKQLTVSKRFS
Cbr-AIR-2      ISGGVEHQLEREIEIQSHLQHPNIIRLYNYFWDAKKIYLILEYAPGGEMYKQLTTQKRFT
Cre-AIR-2      ISGGVEHQLEREIEIQSHLHHPNIVRLYTYFWDAKKIYLVLEYAPGGEMYKSLTNQKRFT
Cbn-AIR-2      ISGSVEHQLEREIEIQSHLHHPNIIRLYTYFWDAKKIYLVLEYAPGGEMYKKLTTERRFS
               ***.***************.****::**.**********:***********.** .:**:

Cel-AIR-2      EPTAAKYMYEIADALSYCHRKNVIHRDIKPENLLIGSQGELKIGDFGWSVHAPSNKRQTM
Cbr-AIR-2      EAMAGKYMYEIADALSYCHRKNVIHRDIKPENLLIGAQGELKIGDFGWSVHAPSNKRQTM
Cre-AIR-2      EVMAGKYMYEIADALQYCHHKKVIHRDIKPENLLIGPQGELKIGDFGWSVHAPSNKRQTM
Cbn-AIR-2      EPTAGKYMYEIADALSYCHRKNVIHRDIKPENLLIGTLGELKIGDFGWSVHAPSNKRQTM
               *  *.**********.***:*:**************  *********************

Cel-AIR-2      CGTMDYLPPEMVNGADHSDAVDLWAIGVLCYEFLVGKPPFEHEDQSKTYAAIKAARFTYP
Cbr-AIR-2      CGTMDYLPPEMVNGNSHSDAVDLWAIGVLCYEFLVGKPPFEHENQADTYSAIKAGRFTYP
Cre-AIR-2      CGTMDYLPPEMIVGNHHSDAVDLWAIGVLCYEFLVGKPPFEHDKQADTYSAIKVARFSYP
Cbn-AIR-2      CGTMDYLPPEMVQGMAHSDAVDLWAIGVLCYEFLVGNPPFEHENQGDTYSAIKEAKFDYP
               ***********: *  ********************:*****:.*..**:*** .:* **

Cel-AIR-2      DSVKKGARDLIGRLLVVDPKARCTLEQVKEHYWIQGMMEAKIRAEKQQKIEKEASLRNH-
Cbr-AIR-2      DFVKKGARDLIGKLLVVDPRRRCSLQEVKDHYWVTSMLDSCRRAAEKQKAERAASLRDH-
Cre-AIR-2      DYVKKGARDLIGKLLVVDPTKRCTLQKVKDHYWVTQMVETARKVAEQAKAEKAASLRDH-
Cbn-AIR-2      DYIKKGARDLIGKLLVIDPKKRISLEQVKTHYWVEMMVETRRRAEQREAGGTKTRQSTRL
               * :*********:***:**  * :*::** ***:  *:::  :. ::      :    :

Cel-AIR-2      -------
Cbr-AIR-2      -------
Cre-AIR-2      -------
Cbn-AIR-2      QMKSIGS
```

C. SYP-1

```
Cel-SYP-1      ------------------------------------------------------------
Cbr-SYP-1      ------------------------------------------------------------
Cre-SYP-1      ------------------------------------------------------------
Cbn-SYP-1      MEKKTPKHWHKDVTHQVTSADLPPTRTDPAEPTSQGSVSSGSSASSTTPPSALTPQPRTI

Cel-SYP-1      ------------------------------------------------------------
Cbr-SYP-1      ------------------------------------------------------------
Cre-SYP-1      ------------------------------------------------------------
Cbn-SYP-1      DISSEYYGGTSIDGCLSSTTPAMFTYTPPTASTSLPLIEIASAVAFRLSAIVAANQSAFP

Cel-SYP-1      ------------------------------------------------------------
Cbr-SYP-1      ------------------------------------------------------------
Cre-SYP-1      ------------------------------------------------------------
Cbn-SYP-1      VYSSLSLPSTSTSSSATSSTSSEELKLMFKGQDILNTDPKFLMDKDNIIRKLQVELRKKT

Cel-SYP-1      --------------MDNFTIWVDA-----------------------------------
Cbr-SYP-1      --------------MDNFTIWVDSA----------------------------------
Cre-SYP-1      --------------MDNFTIWVDA-----------------------------------
Cbn-SYP-1      IKFNDAYKGFNELRLEKSNAWKTLQETEGDVKMETKKKEKPSASKRKVGEEAGSSQKRTK
                             ::: . *

Cel-SYP-1      ------------P----------TEALIETPVDDQSSGFLRDEIML--------------
Cbr-SYP-1      ------------P----------SETITEAPVDDESNSILRKEIQQ--------------
Cre-SYP-1      ------------P----------SEALIETPLDDESNCFLREEIQQ--------------
Cbn-SYP-1      QDEETTKSVSLAPSSSNTSTEDSSPAITPPPANTNSSNSAQQGLDAKTGESKKLAEEKKK
                           *          : ::   * : :*.   :. :

Cel-SYP-1      -------T--------------------------------------QQY---VLEKLDEQ
Cbr-SYP-1      -------T--------------------------------------QQY---VIGKLNEQ
Cre-SYP-1      -------T--------------------------------------QQY---VIEKLDEQ
```

```
Cbn-SYP-1      LEEEVKSLKMKVAENQETATTSSAELRELRGSFDRKNKEMGEVTRQNMRMKEKIKELEDH
                                                         :      : :*:::

Cel-SYP-1      T--EQDKGEQTDE----QAAKSRELASQVQTESQRMHDIKKELNVFKESCKSIELQLVSV
Cbr-SYP-1      ETNEKEKGDHSKE----KTM---KVFKMITTQEKKLVNVSLHLESLEKVCKSIELQLIAM
Cre-SYP-1      KNCEQEKGEQTDE----ETTKASKILSLVTTEGKRSKDISRELVDLQEACKLNEIQLVSI
Cbn-SYP-1      LKEEKEKNKKQDEGTNPQPAKLEEFRGNLTKKNEELTHRNVE----------LENQMEEL
                  *::* .: .*    :     :.   : .: :.  . . .           * *:  :

Cel-SYP-1      KKSIPDRTKLQS--GEKEKSLNEADYELSKFEDLLSSRERELTKIIQRE------QSRNN
Cbr-SYP-1      KESFPESISLTE--EFYEKDLLHVENQIVLLQEICDSRVKTLNQLELNG------FNHSK
Cre-SYP-1      QKNSPDFVKLCK--ENYDQDLIETNNALILLHDNFTKRQSSLNKLQQAG------LSCDK
Cbn-SYP-1      KKELQEEKKKNENQEEEITSLKKDNFELKIANRVCTEDWQRGGKLLSESDRQLLAERKIT
               ::.  :  .  .       .* . :  :   .    .      ::              .

Cel-SYP-1      GEAKNECKRLREMI----------------MAAKQKHEKLVELNSSCAMMQAKYDEMIIR
Cbr-SYP-1      EDAKLECKKLRESI----------------LAAKQKHEKLVTLNVSKIKLQAEKDELISL
Cre-SYP-1      EEAKKECKKLRSCV----------------LEAKQKHEKLLTLRGSVSKLKNEFDEAMTR
Cbn-SYP-1      EELKAENQRLKGALNQIQTSSHLSASATLRRELEQEKQKVNQLKGRFATLEKDYNEKMKL
                : * * ::*:  :                   :*:::*:  *.     :: . :* :

Cel-SYP-1      QDQDREALEEGKLNLKASEEKLEQMREDCVTLRSQLFQFEASRSQDKTTEIEKEIEKITA
Cbr-SYP-1      NNQEAEAIEAAKLVLKSDQELAEKMTEECVSLRSQLVQMEAAQSNNQDGADKLEIDRLQK
Cre-SYP-1      QKKERESIEKARAELKNDQDLVNKMTEECVNLRSQLVQIEAAQSQNQVEADQMEVQRLQN
Cbn-SYP-1      LEEKEK----------------------------------------QAVADKTKIADLQN
               .:. :                                       :    : ::  :

Cel-SYP-1      ETAKVRVENEQLKASLSKIKEDTKILKLKYEARQQEDIENKKLIEER----KRS------
Cbr-SYP-1      KIEQIRQETDGITSKLSEVRKETEEAQKKLNEQKQTEADNQALMGKL----KAD------
Cre-SYP-1      HAKKIRQETEELIPILSKIENDTKEAQKAVEVRRQNELNDEELIKTK----KEA------
Cbn-SYP-1      SNSAFYDQARRLSADLKEEKKKVENLGKELEEERRKAAEKEERVKELEKELKDSQTAHEV
                   .  :   :   *.: .:..:      : .::   :.:  :       *

Cel-SYP-1      IIELLRRKIAEKKKSNTVKGSDRKKITSLKKAIAKEQEKLEKGKKELEQ-LQS-S-----
Cbr-SYP-1      IVALLQKKIEEEKDKK-KRKPELQKMIELKKAISIENLALEQARKELEE-IQVGG-----
Cre-SYP-1      IAKILLQKIQHETKKS-TKNMNLKKIVDLKRAISKESLVLANANKVLDE-MKPDN-----
Cbn-SYP-1      KIEELDQKIKSLEQNAAKKE---AKIKELHDELETRNNSLNAKEGELKRKIEDHKRVVIE
                   * :**    ..   :     *: .*:  :  ..  *   .  *.. ::

Cel-SYP-1      --KTESDLEEEISAMQLEINDYDKQIKDAAKEHEKLFNQIKEQRAANGD------QFNDT
Cbr-SYP-1      --KTVSELKSEITKMQSEIRSYEREIKKATKENEKLIEQIAEIRIPSPDTTLQ--FLNDT
Cre-SYP-1      --KTVNELKREISVMRSEIRGYEKEIREATKENGKLIEQIAEMRTPSPEATSPRMNLNDT
Cbn-SYP-1      KDNEIRSLRDELAKKGVEVKGKEGEIEEKDNQIKKLQMDLDESKKALNS-----------
                 :   .*. *::    *:.  : :*..  ::  **  :: * :    .

Cel-SYP-1      IDIVESDYSDRVVPPQPSVEVTPVHRQVSHDVFS-APLMTSTPLTAATRPL----KRT-R
Cbr-SYP-1      AEIDESEYSQQVVTPKLEINVTPIQRAISRDVFTGAPLMTSTPLHKPEP-T----GKTRA
Cre-SYP-1      VDFNESEYSEQMAIPEPIVNITPVQRIVSHDVFTGAPLMTSTPLPKTAETS----VKTRA
Cbn-SYP-1      -----KELERRAMERK--------HEEMVTKFVTGDKELKD-ALEEARNSLVDSEKKRKA
                    .: . :    :        :. :  ...:    :..  *            :

Cel-SYP-1      AAD--------------------------------RLKTRAEAHT-------AD---VRR
Cbr-SYP-1      AAR--------------------------------RLEQNAKAKT-------AE---LRK
Cre-SYP-1      AAR--------------------------------RLEQTAATKT-------AE---IRK
Cbn-SYP-1      EADQHQRKLLEKEREVENLRKALEEANGSLVASENEVKTEADQHQRKLLEKDKEIEKLRK
                *                                 .::  *  :         :   :*:

Cel-SYP-1      KRGGKK------------------------------------------------------
Cbr-SYP-1      KRGGKK------------------------------------------------------
Cre-SYP-1      KRGGKK------------------------------------------------------
Cbn-SYP-1      ELQDKENANREALEKKEKELQDVKKAQDEEIAQELALLKKDYKYACAKVEFVENKNTEKD
               :   *:
```

```
Cel-SYP-1      ------------------
Cbr-SYP-1      ------------------
Cre-SYP-1      ------------------
Cbn-SYP-1      AELERLKNENAELKSSLH
```

D. SYP-2

```
Cel-SYP-2      --------------------------------MNSAHRSSLKKRPGPQDD-RRVSFASPV
Cbr-SYP-2      --------------------------------MSSTPRSSLKKRPGNPDD-RRVSFATPL
Cbn-SYP-2      MLAESLATSWRTLGSLLMIMVGPETYPSVLPGMSAKPRSSLKKGSGAPDDNRRVSFASPL
                                                *.:  ******  *  ** ******:*:

Cel-SYP-2      SSSQKTAAVTVAAQTKQPAKAKNLRTMHSTPKKSKPAHDVADIISLVSKQSDILDDVSEI
Cbr-SYP-2      SSDQVVDPS----ANKLVENTKNAKLNHPLAKKSKPADDFVDFISLANKQSEVVQKISEL
Cbn-SYP-2      SSDKKDSSA----HRNDHSITKVVKANRPVVKKSKPADEFVDIISLVNHQSEVIEEIFEM
               **.:           :    :*  :  :   ******.:..*:***..:**::::.: *:

Cel-SYP-2      EHKMIKQAKMTQDLTMELANSIERIANMALAESKLSDQMEKQSKKLISLEGKTKELVEKA
Cbr-SYP-2      ESKITKQSAMAKDLTSQLTNFIELIGNVSSSQTRVKSRLEEQSTKLASTEENIAGLVSKA
Cbn-SYP-2      ESKFAKQSAMTQNLTIDLANFIESIAKLSSDSTKVESQLEELSARVANLETNISDLISQA
               * *: **: *:::** :*:* ** *.:::  .::::..::*: * :: . * :   *:.:*

Cel-SYP-2      NNWSKTLENRVDARSHHSTCLNDVQAAIKIINNAKINNDGFSEDFSAHYDKLLDLVETLE
Cbr-SYP-2      DSMCKTFEERKTARAEYSAGLAELQAAIAYVNCKSIENT---TETIGEYDKMLEIVSKIE
Cbn-SYP-2      SSVCAKYESRIDARSQYSTYLLDLQKAFNAINCVKVGNP---EDSHIDYDPLLKIVDQLE
               .. . . *.*  **:.:*: * ::* *:  :*  .: *     :   .** :*.:*. :*

Cel-SYP-2      PWADKL
Cbr-SYP-2      TLVDRF
Cbn-SYP-2      ACVDKF
                 .*::
```

Figure S1. Predicted *Caenorhabditis* protein alignments

The Clustal Omega program {Sievers, 2011 #155} was used to perform protein alignments with predicted protein sequence of *C. elegans*, *C. briggsae*, *C. remanei* and *C. brenneri* **(A)** RAD-51, **(B)** AIR-2, **(C)** SYP-1 and **(D)** SYP-2. Arrow indicates alternative start site of *Cel*-RAD-51 (RAD-51S; {Rinaldo, 1998 #157}. Yellow highlight denotes the *C. elegans* sequence used for antibody production, green highlight is the identical sequence in the other species where the antibody recognized the protein and cyan is the identical sequence in the other species where the antibody did not recognize the corresponding protein. Immunogen for generation of rabbit anti-RAD-51 is indicated; rat anti-RAD-51 was generated from the complete RAD-51S protein sequence {Rosu, 2013 #116}. SYP-2 sequence was not identified in *C. remanei* by either wormbase or NCBI BLAST. * = identical sequence; : = strongly similar; . = weakly similar.

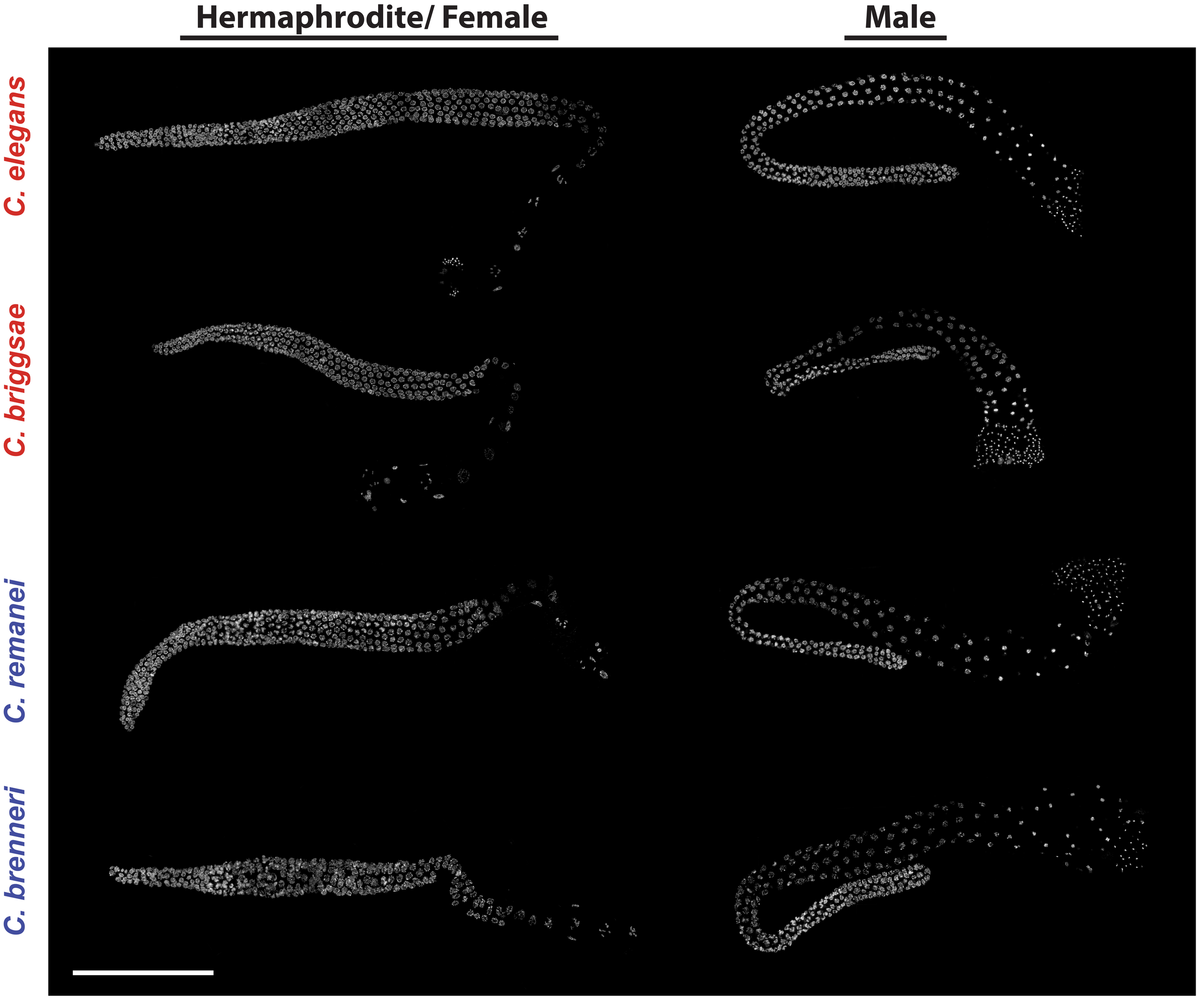
Hermaphrodite/ Female
Male
C. elegans
C. briggsae
C. remanei
C. brenneri

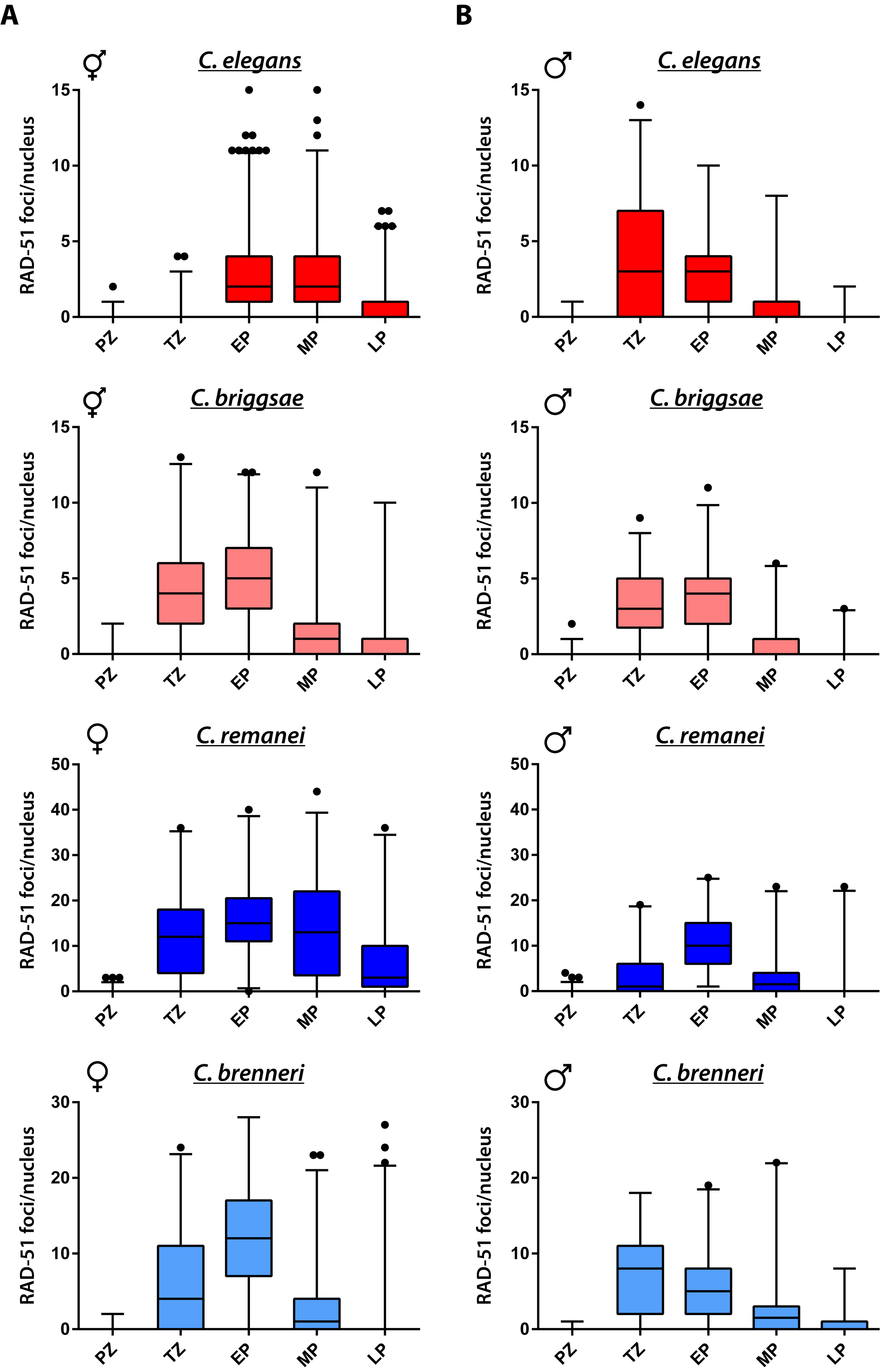
A
B
C. elegans
C. briggsae
C. remanei
C. brenneri
RAD-51 foci/nucleus
PZ
TZ
EP
MP
LP

A ⚥

PZ	*C.elegans*	*C. briggsae*	*C. remanei*	*C. brenneri*
C.elegans		ns	ns	ns
C. briggsae	ns		ns	ns
C. remanei	ns	ns		ns
C. brenneri	ns	ns	ns	

TZ	*C.elegans*	*C. briggsae*	*C. remanei*	*C. brenneri*
C.elegans		$p < 0.0001$	$p < 0.0001$	$p < 0.0001$
C. briggsae	$p < 0.0001$		$p < 0.0001$	$p < 0.01$
C. remanei	$p < 0.0001$	$p < 0.0001$		$p < 0.0001$
C. brenneri	$p < 0.0001$	$p < 0.01$	$p < 0.0001$	

EP	*C.elegans*	*C. briggsae*	*C. remanei*	*C. brenneri*
C.elegans		$p < 0.0001$	$p < 0.0001$	$p < 0.0001$
C. briggsae	$p < 0.0001$		$p < 0.0001$	$p < 0.0001$
C. remanei	$p < 0.0001$	$p < 0.0001$		$p < 0.0001$
C. brenneri	$p < 0.0001$	$p < 0.0001$	$p < 0.0001$	

MP	*C.elegans*	*C. briggsae*	*C. remanei*	*C. brenneri*
C.elegans		$p < 0.01$	$p < 0.0001$	ns
C. briggsae	$p < 0.01$		$p < 0.0001$	$p < 0.05$
C. remanei	$p < 0.0001$	$p < 0.0001$		$p < 0.0001$
C. brenneri	ns	$p < 0.05$	$p < 0.0001$	

LP	*C.elegans*	*C. briggsae*	*C. remanei*	*C. brenneri*
C.elegans		ns	$p < 0.0001$	ns
C. briggsae	ns		$p < 0.0001$	ns
C. remanei	$p < 0.0001$	$p < 0.0001$		$p < 0.0001$
C. brenneri	ns	ns	$p < 0.0001$	

B ♂

PZ	*C.elegans*	*C. briggsae*	*C. remanei*	*C. brenneri*
C.elegans		ns	ns	ns
C. briggsae	ns		$p < 0.05$	ns
C. remanei	ns	$p < 0.05$		$p < 0.05$
C. brenneri	ns	ns	$p < 0.05$	

TZ	*C.elegans*	*C. briggsae*	*C. remanei*	*C. brenneri*
C.elegans		ns	ns	$p < 0.0001$
C. briggsae	ns		ns	$p < 0.0001$
C. remanei	ns	ns		$p < 0.0001$
C. brenneri	$p < 0.0001$	$p < 0.0001$	$p < 0.0001$	

EP	*C.elegans*	*C. briggsae*	*C. remanei*	*C. brenneri*
C.elegans		ns	$p < 0.0001$	$p < 0.0001$
C. briggsae	ns		$p < 0.0001$	$p < 0.01$
C. remanei	$p < 0.0001$	$p < 0.0001$		$p < 0.0001$
C. brenneri	$p < 0.0001$	$p < 0.01$	$p < 0.0001$	

MP	*C.elegans*	*C. briggsae*	*C. remanei*	*C. brenneri*
C.elegans		ns	$p < 0.0001$	$p < 0.0001$
C. briggsae	ns		$p < 0.0001$	$p < 0.0001$
C. remanei	$p < 0.0001$	$p < 0.0001$		ns
C. brenneri	$p < 0.0001$	$p < 0.0001$	ns	

LP	*C.elegans*	*C. briggsae*	*C. remanei*	*C. brenneri*
C.elegans		ns	ns	ns
C. briggsae	ns		$p < 0.05$	ns
C. remanei	ns	$p < 0.05$		ns
C. brenneri	ns	ns	ns	

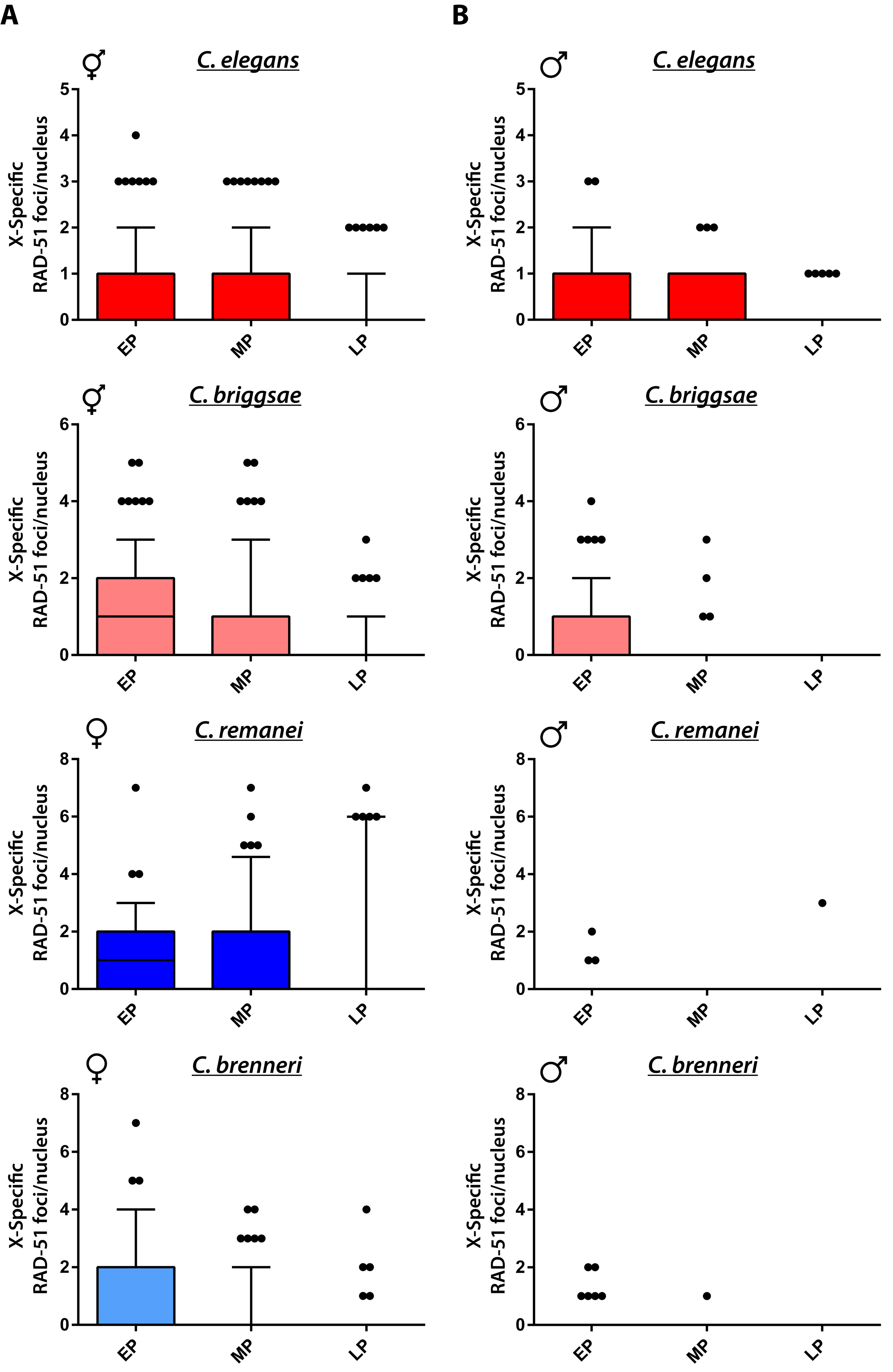
A
B
C. elegans
C. briggsae
C. remanei
C. brenneri
X-Specific RAD-51 foci/nucleus
EP
MP
LP

RAD-51 on X to Autosome Ratio - Statistical Comparison

A

Males	*C. elegans*	*C. briggsae*	*C. remanei*	*C. brenneri*
C. elegans		ns	$p < 0.0001$	$p < 0.0001$
C. briggsae	ns		$p < 0.0001$	$p < 0.0001$
C. remanei	$p < 0.0001$	$p < 0.0001$		ns
C. brenneri	$p < 0.0001$	$p < 0.0001$	ns	

B

Herm/Females	*C. elegans*	*C. briggsae*	*C. remanei*	*C. brenneri*
C. elegans		ns	$p < 0.01$	ns
C. briggsae	ns		$p < 0.0001$	$p < 0.01$
C. remanei	$p < 0.01$	$p < 0.0001$		ns
C. brenneri	ns	$p < 0.01$	ns	

C

	Males vs. Hermaphrodites/Females
C. elegans	$p < 0.01$
C. briggsae	ns
C. remanei	$p < 0.0001$
C. briggsae	$p < 0.0001$

Average Number of RAD-51 on X Chromosome(s) - Statistical Comparison

D

Males	*Cel: 0.33 ± 0.045*	*Cbr: 0.25 ± 0.045*	*Cre: 0.028 ± 0.015*	*Cbn: 0.033 ± 0.013*
Cel: 0.33±0.045		ns	$p < 0.0001$	$p < 0.0001$
Cbr: 0.25 ± 0.045	ns		$p < 0.0001$	$p < 0.0001$
Cre: 0.028 ± 0.015	$p < 0.0001$	$p < 0.0001$		ns
Cbn: 0.033 ± 0.013	$p < 0.0001$	$p < 0.0001$	ns	

E

Herm/Females	*Cel: 0.37 ± 0.024*	*Cbr: 0.65 ± 0.043*	*Cre: 0.99 ± 0.084*	*Cbn: 0.58 ± 0.050*
Cel: 0.37 ± 0.024		$p < 0.0001$	$p < 0.0001$	$p < 0.001$
Cbr: 0.65 ± 0.043	$p < 0.0001$		$p < 0.001$	ns
Cre: 0.99 ± 0.084	$p < 0.0001$	$p < 0.001$		$p < 0.0001$
Cbn: 0.58 ± 0.050	$p < 0.001$	ns	$p < 0.0001$	

F

	Males vs. Hermaphrodites/Females
C. elegans	ns
C. briggsae	$p < 0.0001$
C. remanei	$p < 0.0001$
C. briggsae	$p < 0.0001$

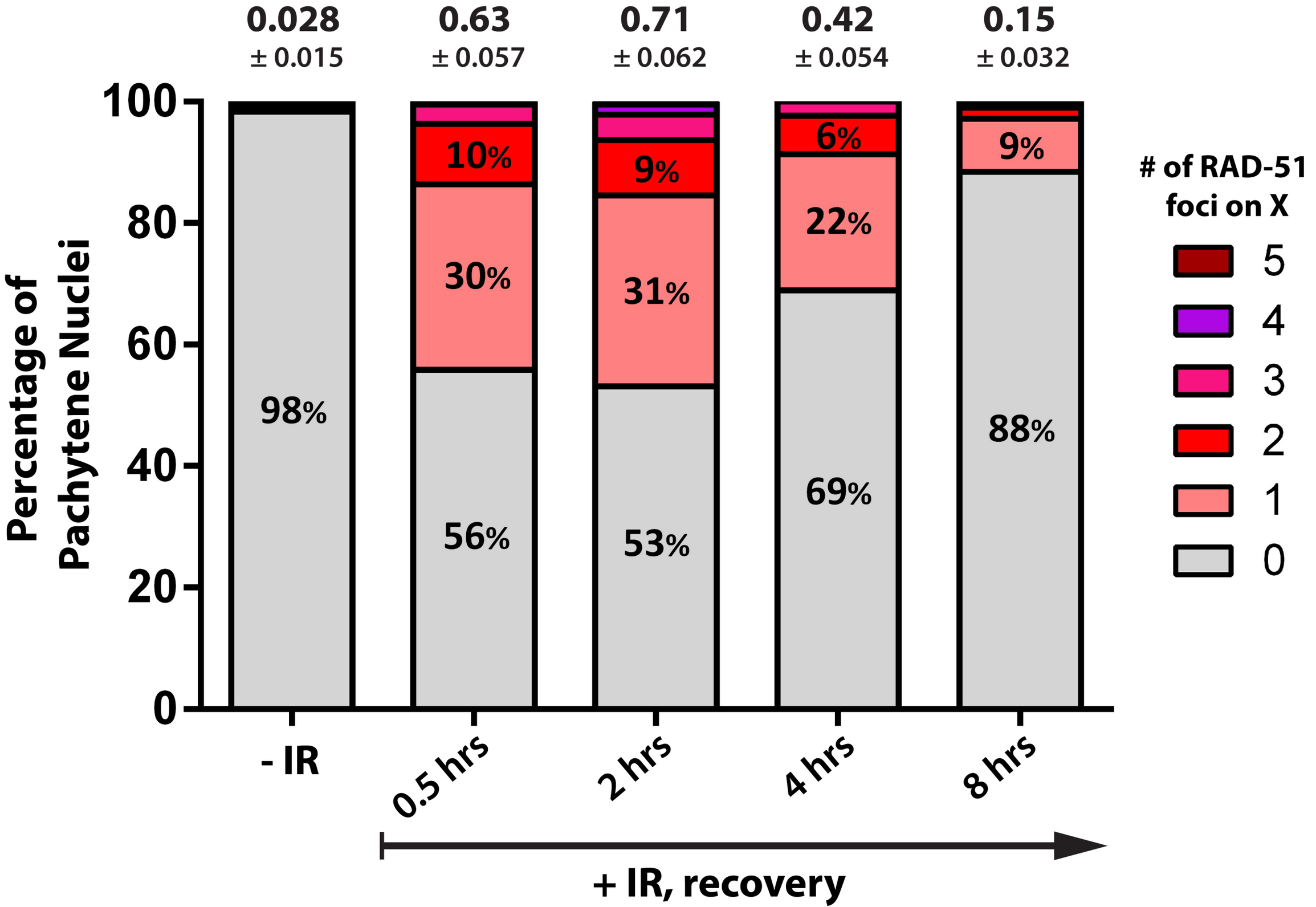
0.028
± 0.015
0.63
± 0.057
0.71
± 0.062
0.42
± 0.054
0.15
± 0.032
Percentage of Pachytene Nuclei
100
80
60
40
20
0
98%
10%
30%
56%
9%
31%
53%
6%
22%
69%
9%
88%
- IR
0.5 hrs
2 hrs
4 hrs
8 hrs
+ IR, recovery
# of RAD-51 foci on X
5
4
3
2
1
0

Table S1. Primer sequences used to construct *C. briggsae and C.remanei* RNAi feeding vectors by two piece Gibson assembly.

Name	**Sequence (5'-3')**
Cbr-spo-11 Forward L4440 overhang	AATTCGAGCTCCACCGCGGTCGGGCGATGTTAAATGTGGT
Cbr-spo-11 Reverse L4440 overhang	CTAGTTCTAGAGCGGCCGCCGCTCAGTGTCAGAATCCGCA
L4440 Forward *Cbr-spo-11* overhang	TGCGGATTCTGACACTGAGCGGCGGCCGCTCTAGAACTAG
L4440 Reverse *Cbr-spo-11* overhang	ACCACATTTAACATCGCCCGACCGCGGTGGAGCTCGAATT
Cbr-rad-51 Forward L4440 overhang	AATTCGAGCTCCACCGCGGTCGTTCGAAGAAGTCGGACCA
Cbr-rad-51 Reverse L4440 overhang	CTAGTTCTAGAGCGGCCGCCTCAAGGTACAAACCTCTGAGCA
L4440 Forward *Cbr-rad-51* overhang	TGCTCAGAGGTTTGTACCTTGAGGCGGCCGCTCTAGAACTAG
L4440 Reverse *Cbr-rad-51* overhang	TGGTCCGACTTCTTCGAACGACCGCGGTGGAGCTCGAATT
Cbr-rad-54 Forward L4440 overhang	AATTCGAGCTCCACCGCGGTGGCCAGCAGAGGTACGTAAT
Cbr-rad-54 Reverse L4440 overhang	CTAGTTCTAGAGCGGCCGCCCTGGAGCTGAAGCCGAACTT
L4440 Forward *Cbr-rad-54* overhang	AAGTTCGGCTTCAGCTCCAGGGCGGCCGCTCTAGAACTAG
L4440 Reverse *rad-54* overhang	ATTACGTACCTCTGCTGGCCACCGCGGTGGAGCTCGAATT
Cre-spo-11 Forward L4440 overhang	AATTCGAGCTCCACCGCGGTACAATCGGCAAACTTCACCG
Cre-spo-11 Reverse L4440 overhang	CTAGTTCTAGAGCGGCCGCCGGTCTGCATCAAACAATCCG
L4440 Forward *Cre-spo-11* overhang	CGGATTGTTTGATGCAGACCGGCGGCCGCTCTAGAACTAG
L4440 Reverse *Cre-spo-11* overhang	CGGTGAAGTTTGCCGATTGTACCCGGTGGAGCTCGAATT
Cre-rad-51 Forward L4440 overhang	AATTCGAGCTCCACCGCGGTGTGGAGAGATAGAGAGATGATGG
Cre-rad-51 Reverse L4440 overhang	CTAGTTCTAGAGCGGCCGCCGCGTCCTCAATTCCATGATTAGT
L4440 Forward *Cre-rad-51* overhang	ACTAATCATGGAATTGAGGACGCGGCGGCCGCTCTAGAACTAG
L4440 Reverse *Cre-rad-51* overhang	CCATCATCTCTCTATCTCTCCACACCGCGGTGGAGCTCGAATT